

# Exploiting internal resonance for vibration suppression and energy harvesting from structures using an inner mounted oscillator

H. Karimpour · M. Eftekhari

Received: 24 October 2012 / Accepted: 24 February 2014 / Published online: 5 April 2014  
© Springer Science+Business Media Dordrecht 2014

**Abstract** The flexural vibration of a symmetrically laminated composite cantilever beam carrying a sliding mass under harmonic base excitations is investigated. An internally mounted oscillator constrained to move along the beam is employed in order to fulfill a multi-task that consists of both attenuating the beam vibrations in a resonance status and harvesting this residual energy as a complementary subtask. The set of nonlinear partial differential equations of motion derived by Hamilton's principle are reduced and semi-analytically solved by the successive application of Galerkin's and the multiple-scales perturbation methods. It is shown that by properly tuning the natural frequencies of the system, internal resonance condition can be achieved. Stability of fixed points and bifurcation of steady-state solutions are studied for internal and external resonances status. It results that transfer of energy or modal saturation phenomenon occurs between vibrational modes of the beam and the sliding mass motion through fulfilling an internal resonance condition. This study also reveals that absorbers can be successfully implemented inside structures without affecting their functionality and encumbering additional space but can also be designed to convert transverse vibrations

into internal longitudinal oscillations exploitable in a straightforward manner to produce electrical energy.

**Keywords** Internal resonance · Vibration suppression · Saturation phenomenon · Energy harvesting

## List of symbols

$xyz$	Inertial coordinate system
$u(s, t), v(s, t), w(s, t)$	Beam neutral axis deflection along $x, y$ and $z$ axes
$\xi \eta \zeta$	Principle axes coordinate system of beam cross-section at position $s$
$c_i, i = u, v, w, \phi$	Damping coefficients
$r(t)$	Position of moving mass from the clamped end
$\psi(s, t), \theta(s, t), \phi(s, t)$	Beam neutral axis Euler rotation angles
$m$	Mass of the beam per unit length $l$
$\hat{e}_i, i = x, y, z, \xi, \eta, \zeta$	Unit vector along the $i$ axis
$J_\xi, J_\eta, J_\zeta$	Principal mass moments of inertia
$D_{11}, D_{22}, D_{33}, D_{13}$	Bending and stiffness rigidities
$E_1, E_2, E_3, G_{12}, G_{13}, G_{23}$	Elastic and shear modulus
$\vec{F}_c$	Applied force vector to the moving mass

H. Karimpour (✉)  
Department of Mechanical Engineering, Islamic Azad University, Khomeinishahr Branch, Isfahan, Iran  
e-mail: karimpour@iaukhsh.ac.ir

M. Eftekhari  
School of Engineering, Shahid Bahonar University of Kerman, Kerman, Iran

$m_a$	Moving mass
$Q_i, i = u, v, w, \phi$	External forces
$\vec{v}_m$	Velocity vector of the moving mass
$\vec{r}_m$	Position vector of the moving mass
$\ell(s, t)$	Lagrangian density
$k_a$	Controller gain
$r_e$	Equilibrium position of the moving mass
$k_s$	Nondimensional controller gain

## 1 Introduction

As a promising technology, one profile of energy harvesting consists of exploiting nonlinear properties of vibrational structures for capturing useful energies provided by environmental sources or machines operation. The specific longitudinal implementation and design of the companion device is purposed to deviate the energy transmitted to the main structure into a useful form. The range of motion can reach large amplitudes so that nonlinearity get involved in and could improve efficiency upon other existing harvesters limited to linear principles. Another attribute of the proposed system consists of the feasibility to be compactly installed inside the framework of the structure and it consequently won't occupy extra space or interfere in the main system's normal operation. By tuning the parameters adequately, this system will react to transverse excitations by transferring the energy to a longitudinal mode of motion. This property is the principle that we will take advantage through this article. Ambient energy harvesting has been the subject of numerous researches purposed for realizing an autonomous solution to power small-scale electronic mobile devices. Due to the almost universal presence of mechanical vibrations from eccentric machine shaking to human movements and ambient sounds, vibration energy harvesting can play a major role in providing an alternate source of energy. Nonetheless, most approaches are mainly based on piezoelectric materials or resonant linear oscillators that are acted on by ambient vibrations but don't generate considerable amount of power. Here is proposed a new method based on the exploitation of large amplitude oscillations which introduced the study into the nonlinear domain. More exactly, this research

relies on the saturation phenomenon which will permit to attenuate the vibration of the flexural modes by translating the energy to the longitudinally mounted sliding oscillator. There are also potential applications to such combination of primary and secondary systems; As vibrations come in a vast variety of forms from sources as diverse as wind induced movements, one attempt is to converse this form of energy into electrical one by twisting a coil circuit around the beam profile through which a magnet mass is made to oscillate, inducing an electrical current in the circuit. Many working solutions for vibration-to-electricity conversion are based on oscillating mechanical elements that convert kinetic energy via capacitive, inductive or piezoelectric methods. The present method, while suppressing the vibration of one mode, simultaneously permits electric power generation via the other useful mode.

### 1.1 Related works

Many structural elements can be modeled as flexible beams carrying a moving mass, such as vehicles crossing over bridges, cranes transporting materials along their boom, to mention a few, and may found applications as active absorbers sliding along robotic arms in space missions. Many researchers have investigated the dynamic and nonlinear response of these elements in the last few decades which resulted in a considerable amount of literature. In what follows are enumerated some aspects of these related works.

Zovandey and Nayfeh [1] investigated the nonlinear response of a cantilever beam carrying a lumped mass under parametric base excitation. The lumped mass was located at an arbitrary position and governing equations was solved using Galerkin method and the perturbation method of multiple scales. Frequency and force-responses were obtained from the modulation equations and were in good agreement with the experimental results carried out by authors. Some of the linear and nonlinear analyses of beam-mass interaction systems are presented in refs. [2–6].

Dynamic stability of continuous systems under moving loads was presented by Kononov and Borst [4] and Verichev and Metrikine [5]. In a separate study, Siddiqui et al. [6–8] considered a more general case where the moving mass has an additional degree-of-freedom instead of prescribed motion. Golnaraghi [9, 10] proposed the moving mass as a controller to suppress

vibrations in a beam. When the natural frequency of this integrated controller is set to one-half or one-third of the resonant mode frequency, the nonlinear coupling creates a unidirectional energy-transfer mechanism leading to the response saturation in the excited mode or suppression of its vibrations via internal resonance. Internal resonance may occur in systems if the linear natural frequencies  $\omega_i$  are commensurate or nearly commensurate; that is  $\sum_{i=1}^n k_i \omega_i \approx 0$ , where  $k_i$  are positive or negative integers. When the nonlinearity in the system is cubic, internal resonance of order four may occur; that is,  $\omega_n \approx \omega_m$ ,  $\omega_n \approx 3\omega_m$ ,  $\omega_n \approx |\pm 2\omega_m \pm \omega_k|$ , or  $\omega_n \approx |\pm \omega_m \pm \omega_k \pm \omega_l|$ . When the nonlinearity is quadratic, third-order internal resonances may occur if  $\omega_n \approx 2\omega_m$ ,  $\omega_n \approx \omega_m \pm \omega_k$  [11].

In Ref. [8], large oscillation motion of a cantilever beam carrying a spring-mass system was investigated using time-frequency analysis. The equations of planar motion were solved combining average acceleration and iterative methods and the system exhibited internal resonance. In their study, the equations were discretized using Galerkin method and particular assumptions have been made on the moving mass motion about its equilibrium position. In the works cited earlier [6, 7], the same problem has been investigated using combination of numerical and perturbation methods. In that research, the nonlinearities arose merely due to the coupling between the beam and the mass, evaluated near the equilibrium position of the vibrating mass. Due to quadratic nonlinear coupling terms, the system exhibited the 2:1 internal resonance condition. Both [6, 7] and [8] investigated free vibrations of the beam.

Mechanical oscillators are usually designed to be resonantly tuned to the ambient dominant frequency. One major drawback to the linear energy harvesting approach is that it assumes most of the ambient vibration is concentrated at a dominant frequency while in reality the energy spectra of the available vibration are commonly spread in a broadband frequency range, with the prevalence of low frequency components. Tuning the oscillators is not always possible due to geometrical/dynamical constraint but in recent papers [12–15], interesting methods have been proposed to increase harvesters bandwidth, almost all by considering nonlinear oscillators instead of linear resonant ones. Furthermore unlike linear harvesters, nonlinear oscillators can have multiple stability regions and basins of attraction that may be exploited for harvesting purposes.

An important question that must be addressed by any energy harvesting technology is related to the transduction mechanism generating electrical energy from motion. Such mechanical device is designed with the aim of maximizing the coupling between the kinetic energy source and the transduction mechanism which consists of electromagnetic induction or strain piezoelectric interaction. Researchers in [13] presented a nonlinear electromagnetic energy harvesting device that has a broadly resonant response. The harvester is modeled using a Duffing-type equation under both pure-tone and narrow-band random excitations which showed that in addition to the primary resonance, the superharmonic resonances of the harvester may be useful in converting mechanical to electrical energy. Authors in Ref. [16] modeled the nonlinear behavior of an electromagnetic harvester sustaining oscillations through the phenomena of magnetic levitation by Duffing's equation, and confirmed by direct numerical integration a broadband frequency response for the nonlinear harvester.

As different forms of extractable energy are available, [17] exploited the concept of galloping of square cylinders to harvest wind energy through a piezoelectric transducer attached to the transverse degree of freedom. They determined the onset of galloping which appears as a Hopf bifurcation through linear analysis. Ref. [18] investigated energy harvesting from vortex-induced vibrations. Linear analysis determined the effect of the electrical load resistance of the transducer on the natural frequency of the cylinder and the onset region of synchronization between shedding and the cylinder oscillating frequency. Researchers in Ref. [19] implemented a velocity feedback to reduce the flutter speed of a rigid airfoil to any desired value, enabling to produce limit-cycle oscillations at low wind speeds. The nonlinear spring coefficients were selected so to produce supercritical Hopf bifurcations, increasing the amplitudes of the ensuing limit cycles and hence the harvested power. Researchers in Ref. [20] developed a nonlinear distributed-parameter model for a piezoelectric cantilever beam with a tip mass as an energy harvester under parametric excitation. The method of multiple scales is used to obtain analytical expressions for the tip deflection, output voltage, and harvested power near the first principal parametric resonance. Results show that a one-mode approximation in the Galerkin approach is not sufficient to evaluate the performance of the harvester. In [21], a piezoelectric patch on a ver-

tically mounted cantilever beam with a tip mass that is excited in the transverse direction at its base is proposed as an energy harvesting device. By enabling the beam to buckle by selecting large tip masses, nonlinear behavior in the system dynamics may include multiple solutions. Jumps between buckled configurations are exploited as a harvesting mechanism demonstrating low natural frequencies, a high level of harvested power and an increased bandwidth over a linear harvester.

### 1.2 Current prototype

In the present work, the forced vibration of a three-dimensional composite beam carrying an axially moving mass retained by a spring is investigated throughout a nonlinear oscillation regime, see Fig. 1. The internal mass is influenced by the beam acceleration and flexural motion and is restored to equilibrium by a linear spring along the beam arc length. The specific implementation of the companion harvesting device along the structure longitudinal dimension permit to deviate the transversal vibration energy transmitted from exter-

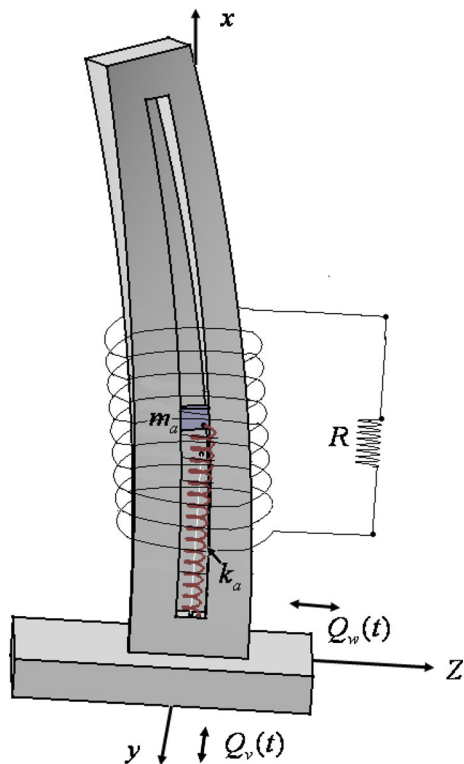


**Fig. 1** Schematic of composite cantilever beam consisting mass-spring system

nal sources into an exploitable form. By tuning the parameters adequately, this system will react to transverse excitations by transferring the energy to a longitudinal mode of motion.

Equations of motion for a composite beam obtained by Pai [22,23] and Arafat [24] are extended here by considering an additional mass sliding along it. Resulting nonlinear partial differential equations of motion are reduced to a set of ordinary differential equations using Galerkin method by considering eigenfunctions of an unequipped composite beam. These equations are then solved using the approximate perturbation solution for two-to-one or one-to-one internal resonance and external resonance conditions. Linear and nonlinear quadratic or cubic terms are evaluated at the equilibrium position of the moving mass. Three modulation equations describing the dynamics of interacting modes are obtained. Exchange of energy between the beam and the moving mass occurring through the internal resonance and saturation phenomenon are exhibited in form of frequency response and force response diagrams [25]. It is shown how multi-branched nontrivial response curves exhibit saddle-node and Hopf bifurcations. Moreover, stability and local bifurcation analysis of the problem is carried out for flapwise and chordwise excitations.

### 1.3 Practical issues

As the range of motion can reach large amplitudes, nonlinearity phenomena will intervene that in turn permits to improve efficiency upon other existing harvesters whose functionality is limited to linear ranges of motion. Another attribute of the proposed system consists of the feasibility to be compactly installed within the structure framework and as a consequence, to not occupy extra space or to cause any interference with the normal operation of primary system (see Fig. 2).

The complexity of the modeled system leads to concerns regarding the validation of the model and the assumptions that have been used. For example, in a practical experiment any useful energy harvesting would be accompanied by significant amounts of friction as the mass moves along the (deforming) column. Meanwhile, off-axis motion of the mass (e.g., rattling) would be exaggerated due to the deformation. Using a spherical shaped mass sliding into a cylindrical tube along the structure length may be considered as a plausible solution, minimizing friction and not sensi-

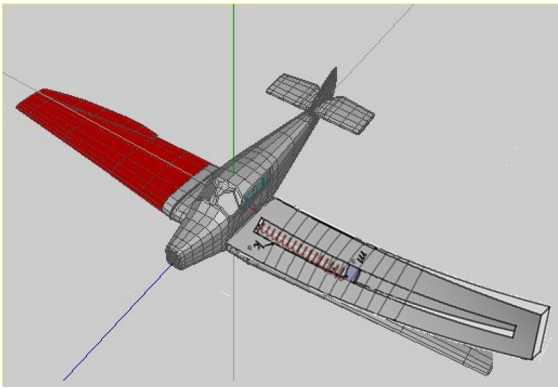


**Fig. 2** An example on how proposed absorber may be installed within the structure framework

tive to the passage curvature. Although increasing the clearance will provoke more rattling effects, nonetheless this will offer a smoother pass of the reciprocating mass through the tube length. Moreover, the spherical mass keeps contact to the interior walls along its circle perimeter, instead of a whole lateral surface in case a cylindrical mass is used. Actually, the primary role of this harvester is to function as an absorber for the transversal vibrations and hence minimizing beam deflections. Thus, off-axis rattling will not be accentuated by external trembles and eventually a steady state can be reached. It is, however, not deniable that no reliable conclusion on the efficiency of proposed apparatus can be achieved without performing actual experiments.

## 2 Derivation of equations of motion

The nonlinear equations of motion for the system which is shown in Fig. 1 can be obtained from the extended Hamilton's principle,

$$\delta I = \int_{t1}^{t2} (\delta L + \delta w_e) dt = 0. \quad (2.1)$$

where  $\delta L$  and  $\delta w_e$  present the variation of the Lagrangian and virtual work of nonconservative forces, respectively. The total Lagrangian is composed of three parts; one part for the composite beam and the other parts for the moving mass and coil which are presented as follows

$$\delta L(t) = \delta L_{beam}(t) + \delta L_{mass}(t) + \delta L_{coil}(t), \quad (2.2)$$

$$\delta L_{beam}(t) = \int_0^l \delta \ell_b(s, t) ds, \quad (2.3)$$

$$\ell_b(s, t) = \frac{1}{2} \left\{ \begin{array}{l} m(\dot{u}^2 + \dot{v}^2 + \dot{w}^2) \\ + (J_\xi \omega_\xi^2 + J_\eta \omega_\eta^2 + J_\zeta \omega_\zeta^2) \\ - \varepsilon^T [k] \varepsilon \\ + \lambda [1 - (1 + u')^2 + v'^2 + w'^2] \end{array} \right\},$$

$$\delta L_{mass}(t) = \int_0^l \delta \left( \frac{1}{2} m_a \vec{v}_m \cdot \vec{v}_m \right) \delta(s - r) ds, \quad (2.4)$$

$$L_{coil}(t) = \frac{1}{2} L_H \dot{q}^2 + \alpha \dot{q}(r - r_e), \quad \delta L_{coil}(t) = L_H \dot{q} \delta \dot{q} + \alpha r \delta \dot{q} + \alpha \dot{q} \delta r, \quad (2.5)$$

In the above terms, the constraint of beam length inextensibility is enforced into the formulation through introducing Lagrange's multiplier  $\lambda(s, t)$ . The Lagrangian of the moving mass consists of its kinetic energy, neglecting the rotary inertia, and depends on its current arc length position  $s = r(t)$  along the deflected beam. The coil portion is computed as Eq. (2.5), in which  $\alpha = 2n\pi R_c B$ , where  $B$  designs the magnetic field intensity,  $n$  the number of coil turns,  $L_H$  the magnetic induction of the coil and  $R_c$  the coil radius. The velocity vector of the moving mass expressed in the inertial coordinate is given by

$$\vec{v}_m = (\dot{u}(s, t) + \dot{r} \cos(\theta) \cos(\psi))_{s=r(t)} \hat{e}_x + (\dot{v}(s, t) + \dot{r} \cos(\theta) \sin(\psi))_{s=r(t)} \hat{e}_y + (\dot{w}(s, t) - \dot{r} \sin(\theta))_{s=r(t)} \hat{e}_z. \quad (2.6)$$

Virtual-work of the nonconservative forces are obtained as

$$\delta w_e = \int_0^l (\vec{F}_c \cdot \delta \vec{r}_m \delta(s - r) + ((Q_u^* - c_u \dot{u}) \delta u + (Q_v^* - c_v \dot{v}) \delta v + (Q_w^* - c_w \dot{w}) \delta w) + (Q_\phi^* - c_\phi \dot{\phi}) \delta \phi) ds - (R_{int} + R_{load}) \dot{q} \delta q \quad (2.7)$$

where  $\vec{F}_c$  is the external force vector applied to the moving mass. Parameters  $c_u, c_v, c_w, c_\phi$  are damping coefficients and  $Q_u, Q_v, Q_w, Q_\phi$  are external forces applied to the beam.  $R_{int}, R_{load}$  are the internal resistance of the coil and the resistance of the external load. The vector  $\vec{r}_m$  is the position vector of moving mass in the inertial coordinate system. The vectors  $\vec{F}_c$  and  $\vec{r}_m$  are expressed in the following equations as

$$\vec{F}_c = f_c\{(\cos(\theta) \cos(\psi))_{s=r(t)}\hat{e}_x + (\cos(\theta) \sin(\psi))_{s=r(t)}\hat{e}_y - (\sin(\theta))_{s=r(t)}\hat{e}_z\}, \tag{2.8}$$

$$\vec{r}_m = (r(t) + u(s, t))_{s=r(t)}\hat{e}_x + (v(s, t))_{s=r(t)}\hat{e}_y + (w(s, t))_{s=r(t)}\hat{e}_z, \tag{2.9}$$

where, in Eq. (2.8),  $f_c = -k_a r(t)$  is the spring restitutive force magnitude and  $k_a$  is the spring constant. Substituting Eqs. (2.2) and (2.7) in Eq. (2.1) and setting each of the coefficients  $\delta u(s, t)$ ,  $\delta v(s, t)$ ,  $\delta w(s, t)$ ,  $\delta \phi(s, t)$  and  $\delta r(t)$  equal to zero, the governing equations of motion and boundary conditions are obtained as

*u variation:*

$$[m\ddot{u} - Q_u^*] + \{m_a(\ddot{u} + \dot{u}'\dot{r}) + m_a\ddot{r} \cos(\theta) \cos(\psi) + m_a\dot{r}(\dot{r}w'w'' + \dot{w}'w') \cos(\psi) - m_a\dot{r}(\dot{r}v'v'' + \dot{v}'v') \cos(\theta) - f_c(\cos(\theta) \cos(\psi))\}_{s=r(t)} = [\lambda(1 + u')] + A_{11} \left(u' + \frac{v'^2}{2} + \frac{w'^2}{2}\right)' + B_{11}(\phi' + v''w') + B_{13}(v'' + \phi w'')' + D_{22}(w'w''')' + D_{33}(v'v''')' + D_{13}(v'\phi'')' - J_\eta(w'\ddot{w}') - J_\zeta(v'\ddot{v}'),$$

*Boundary condition:*

at  $s = 0, u = 0,$

at  $s = L, \lambda(1 + u') = -A_{11} \left(u' + \frac{v'^2}{2} + \frac{w'^2}{2}\right) - B_{11}(\phi' + v''w') - B_{13}(v'' + \phi w'') - D_{22}(w'w''') - D_{33}(v'v''') - D_{13}(v'\phi'') + J_\eta(w'\ddot{w}') + J_\zeta(v'\ddot{v}'), \tag{2.10}$

*v variation:*

$$[m\ddot{v} + c_v\dot{v} + D_{33}v^{iv} + D_{13}\phi''' - J_\zeta\ddot{v}'] + \{m_a(\ddot{v} + \dot{v}'\dot{r}) + m_a\dot{r} \cos(\theta) \sin(\psi) + m_a\dot{r}(w''w' + \dot{w}'w') \sin(\psi) + m_a\dot{r}(\dot{r}v'' + \dot{v}') \cos(\theta)\}_{s=r(t)} - f_c(\cos(\theta) \sin(\psi))_{s=r(t)} = Q_v - D_{11}(\phi'w' + v''w'^2)' - (D_{22} - D_{33})(\phi^2v'' - \phi w'')' - D_{33}[v'(v'v'')' + v'(w'w'')]' + D_{13} \left[\frac{1}{2}(\phi'\phi^2)' - 2(v''w')' - \frac{1}{2}v'^2\phi''\right]$$

$$- (w'w'')'\phi] + J_\xi \frac{\partial}{\partial t}(\dot{\phi}w' + \dot{v}'w'^2)' - (J_\eta - J_\zeta) \left[(v'w'\ddot{w}') - \frac{\partial}{\partial t}(\dot{v}'\phi^2 - \dot{w}'\phi)\right] + J_\zeta(v'\dot{v}^2 + v'\dot{w}^2)' - \frac{m}{2} \left\{v' \left[\int_{-L}^s \frac{\partial^2}{\partial t^2} \int_0^s (v'^2 + w'^2) ds\right] ds\right\}' - \left(v' \int_L^s Q_u ds\right)' + (\lambda v')',$$

*Boundary condition:*

at  $s = 0, v = 0, v' = 0,$

at  $s = L,$

$$D_{33}v'' + D_{13}\phi' = -D_{11}(v''w'' + \phi'w') - (D_{22} - D_{33})(\phi^2v'' - \phi w'' - v'w'w'') + D_{13} \left(\frac{1}{2}\phi^2\phi' - \frac{1}{2}v'^2\phi' - \phi w'w'' - 2v''w'\right),$$

$$D_{33}v''' + D_{13}\phi'' - J_\zeta\ddot{v}' = -D_{11}(\phi'w' + w'^2v'')' - (D_{22} - D_{33})(\phi^2v'' - \phi w'')' - D_{33}[v'(v'v'')' + v'(w'w'')]' + D_{13} \left[\frac{1}{2}(\phi^2\phi') - \frac{1}{2}v'^2\phi'' - \phi(w'w'')' - 2(v''w')'\right] + J_\xi \frac{\partial}{\partial t}(\dot{\phi}w' + w'^2\dot{v}') + (J_\eta - J_\zeta) \frac{\partial}{\partial t}(\phi^2\dot{v}' - \phi\dot{w}') + J_\zeta \left[v' \frac{\partial}{\partial t}(v'\dot{v}') + v' \frac{\partial}{\partial t}(w'\dot{w}')\right], \tag{2.11}$$

*w variation:*

$$[m\ddot{w} + c_w\dot{w} + D_{22}w^{iv} - J_\eta\ddot{w}'] + \{m_a(\ddot{w} + \dot{w}'\dot{r}) + m_a\dot{r} \sin(\theta) - m_a\dot{r}(\dot{r}w'' + \dot{w}') + f_c(\sin(\theta))\} = Q_w + D_{11}(\phi'v'' + v''^2w')' + (\phi'v'' + v''^2w')' + (D_{22} - D_{33})(\phi^2w'' + \phi v'')' - D_{22}(w'(w'w''))' - D_{33}(w'(v'v''))' + D_{13}[v'^2 - (\phi\phi)'] - w'(\phi v'')' - J_\xi(\dot{\phi}\dot{v}' + \dot{v}'^2w') + J_\eta(w'\dot{w}^2)' + J_\zeta(w'\dot{v}^2)' - (J_\eta - J_\zeta) \frac{\partial}{\partial t}[(\dot{w}'\phi^2) + (\dot{v}'\phi)]'$$

$$\begin{aligned}
& - \left( w' \int_L^s Q_u ds \right)' \\
& - \frac{m}{2} \left\{ w' \left[ \int_L^s \frac{\partial^2}{\partial t^2} \int_0^s (v'^2 + w'^2) ds \right] ds \right\}' \\
& + (\lambda w')',
\end{aligned}$$

Boundary condition:

$$\text{at } s = 0, w = 0, w' = 0,$$

$$\text{at } s = L,$$

$$\begin{aligned}
D_{22}w'' &= (D_{22} - D_{33})(\phi^2 w'' + \phi v'') \\
&- D_{13}[\phi \phi' + (\phi v')w'], \\
D_{22}w''' &- J_\eta \ddot{w}' = D_{11}(w'v'^2 + v''\phi') \\
&- D_{22}[w'(w'w'')] - D_{33}[w'(v'v'')] \\
&+ (D_{22} - D_{33})(\phi^2 w'' + \phi v'') \\
&- D_{13}[w'(\phi v'') + (\phi \phi') - v'^2] \\
&- J_\xi (w'\dot{v}^2 + \dot{\phi}v') \\
&+ J_\eta \left[ w' \frac{\partial}{\partial t} (w'\dot{w}') \right] + J_\zeta \left[ w' \frac{\partial}{\partial t} (v'\dot{v}') \right] \\
&- (J_\eta - J_\zeta) \frac{\partial}{\partial t} (\phi^2 \dot{w}' + \phi \dot{v}'), \tag{2.12}
\end{aligned}$$

$\phi$  variation:

$$\begin{aligned}
J_\xi \ddot{\phi} + c_\phi \dot{\phi} - D_{11}\phi'' - D_{13}v''' &= Q_\phi + D_{11}(v''w') \\
&+ (D_{22} - D_{33})(v''w'' - \phi v'^2 + \phi w'^2) \\
&+ D_{13} \left[ \frac{1}{2}(v'^2 v'')' - \frac{1}{2}\phi^2 v''' + v'(w'w'')' + \phi w''' \right] \\
&- J_\xi \frac{\partial}{\partial t} (\dot{v}'w') \\
&+ (J_\eta - J_\zeta)(\phi \dot{v}'^2 - \phi \dot{w}'^2 - \dot{v}'\dot{w}'),
\end{aligned}$$

Boundary condition:

$$\text{at } s = 0, \phi = 0,$$

$$\begin{aligned}
\text{at } s = L, D_{11}\phi' + D_{13}v'' &= -D_{11}(v''w') \\
&+ D_{13} \left( \frac{1}{2}\phi^2 v'' - \frac{1}{2}v'^2 v'' - \phi w'' - v'w'w'' \right), \tag{2.13}
\end{aligned}$$

$r$  variation:

$$\begin{aligned}
\{m_a \ddot{r} + m_a \ddot{u} \cos(\theta) \cos(\psi) \\
&+ m_a \dot{u} \dot{w}' w' \cos(\psi) - m_a \dot{u} \dot{v}' v' \cos(\theta) \\
&+ m_a \ddot{v} \cos(\theta) \sin(\psi) + m_a \dot{v} \dot{w}' w' \sin(\psi) \\
&+ m_a \dot{v} \dot{v}' \cos(\theta) - m_a \ddot{w} \sin(\theta)\}_{s=r(t)} \\
&- m_a \dot{u} \dot{u}' - m_a \dot{v} \dot{v}'
\end{aligned}$$

$$\begin{aligned}
& - f_c (\cos(\theta) \cos(\psi))_{s=r(t)} \\
& - f_c (\cos(\theta) \cos(\psi))_{s=r(t)} u' \\
& - f_c (\cos(\theta) \sin(\psi))_{s=r(t)} v' \\
& - f_c (\sin(\theta))_{s=r(t)} w' - (\alpha \dot{q}) = 0. \tag{2.14}
\end{aligned}$$

$q$  variation:

$$L_H \ddot{q} + (R_{\text{int}} + R_{\text{load}}) \dot{q} + \alpha \dot{r} = 0. \tag{2.15}$$

It is noteworthy that in the derivation of above equations, the variation process for variables  $u, v, w$  was obtained through expression

$$\begin{aligned}
\delta \Delta(s, t) &= \delta \Delta + \frac{\partial \Delta}{\partial s} \delta r \Big|_{s=r(t)}, \\
\Delta &= u, v, w, \dot{u}, \dot{v}, \dot{w} \tag{2.16}
\end{aligned}$$

keeping in mind that it has to reflect the dependence to  $s = r(t)$ . Rotation angles  $\theta, \psi$  are related to beam deflections through kinematics [24] and Eq. (2.10) is solved for the Lagrange multiplier  $\lambda(s, t)$ . The result is

$$\begin{aligned}
\lambda &= J_\eta (w'\ddot{w}') + J_\zeta (v'\ddot{v}') - D_{22}(w'w''') \\
&- D_{33}(v'v''') - D_{13}(v'\phi'') \\
&- B_{11}(\phi' + v''w') - B_{13}(v'' + \phi w'') \\
&- \frac{m}{2} \left\{ \int_L^s \frac{\partial^2}{\partial t^2} \int_0^s (v'^2 + w'^2) ds \right\} ds - \left( \int_L^s Q_u ds \right) \\
&+ \left\{ m_a \ddot{u} + m_a \ddot{r} \left( 1 - \frac{v'^2}{2} + \frac{w'^2}{2} \right) - 2m_a \dot{r} \dot{v}' v' \right. \\
&\left. - f_c \left( 1 - \frac{v'^2}{2} + \frac{w'^2}{2} \right) \right\}_{s=r(t)}, \tag{2.17}
\end{aligned}$$

Eq. (2.17) is then substituted in the underlined terms of Eqs. (2.11) and (2.12). In the next section, the equations are obtained in a nondimensional form.

### 3 Dimensionless equations

The following dimensionless parameters are defined for presenting the equations of motion

$$\begin{aligned}
s^* &= \frac{s}{l}, c_v^* = \frac{c_v l^2}{\sqrt{m D_{33}}}, \\
\beta_{11} &= \frac{D_{11}}{D_{33}}, J_\xi^* = \frac{J_\xi}{m l^2}, Q_v = \frac{l^3}{D_{33}} Q_v, \\
v^* &= \frac{v}{l}, c_w^* = \frac{c_w l^2}{\sqrt{m D_{33}}}, \\
\beta_{22} &= \frac{D_{22}}{D_{33}}, J_\eta^* = \frac{J_\eta}{m l^2}, Q_w^* = \frac{l^3}{D_{33}} Q_w.
\end{aligned}$$

$$\begin{aligned}
 w^* &= \frac{w}{l}, c_\phi^* = \frac{c_\phi}{\sqrt{mD_{33}}}, \\
 \beta_{13} &= \frac{D_{13}}{D_{33}}, J_\zeta^* = \frac{J_\zeta}{ml^2}, Q_\phi^* = \frac{l^2}{D_{33}} Q_\phi, \\
 r^* &= \frac{r}{l}, m_s^* = \frac{m_a}{ml}, k_s^* = \frac{ka l^3}{D_{33}}, \\
 t^* &= \sqrt{\frac{D_{33}}{ml^4}} t, \beta_{33} = 1, Q_u^* = \frac{l^3}{D_{33}} Q_u \\
 k_t^* &= 2n\pi, k_q^* = \frac{L_H}{R_{\text{int}} + R_{\text{load}}} \sqrt{\frac{D_{33}}{ml^4}}, \\
 k_e^* &= \frac{2n\pi(R_c B)^2 l^3}{D_{33}} \frac{1}{R_{\text{int}} + R_{\text{load}}} \sqrt{\frac{D_{33}}{ml^4}} \tag{3.1}
 \end{aligned}$$

Moreover, the forcing terms, damping terms are assumed to be  $O(\varepsilon)$  while ( $\varepsilon \ll 1$ ) is a small dimensionless parameter used as a bookkeeping parameter. Neglecting nonlinear rotary inertia terms, the underlined terms below are those added to the governing equations of the single beam obtained by Arafat [24], hence showing the effect of the moving mass. For ease of notation, the superscript (\*) is dropped and a prime and an over dot is used to denote  $\frac{\partial}{\partial s^*}$  and  $\frac{\partial}{\partial t^*}$ , respectively. The nondimensional equations are obtained as

$$\begin{aligned}
 \ddot{v} + \varepsilon c_v \dot{v} + \beta_{33} v^{iv} + \beta_{13} \phi''' - J_\zeta \ddot{v}'' + m_s \ddot{v} \delta(s-r) \\
 = \varepsilon \left\{ \begin{aligned} & Q_v(t) - [v'(s-1)]' Q_u(t) \\ & + H_v(s,t) + \underline{H_{vj}(s,t)} \end{aligned} \right\}, \tag{3.2}
 \end{aligned}$$

$$\begin{aligned}
 \ddot{w} + \varepsilon c_w \dot{w} + \beta_{22} w^{iv} - J_\eta \ddot{w}'' + m_s \ddot{w} \delta(s-r) \\
 = \varepsilon \left\{ \begin{aligned} & Q_w(t) - [w'(s-1)]' Q_u(t) \\ & + H_w(s,t) + \underline{H_{wj}(s,t)} \end{aligned} \right\}, \tag{3.3}
 \end{aligned}$$

$$\begin{aligned}
 J_\xi \ddot{\phi} + \varepsilon c_\phi \dot{\phi} - \beta_{11} \phi'' - \beta_{13} v'' \\
 = \varepsilon \{ Q_\phi(t) + H_\phi(s,t) \}, \tag{3.4}
 \end{aligned}$$

$$m_s \ddot{r} + k_s r - k_t \dot{q} = \varepsilon \{ H_r(t) \}, \tag{3.5}$$

$$k_q \ddot{q} + \dot{q} + \varepsilon k_e \dot{r} = 0, \tag{3.6}$$

where  $H_{vj}(s, t), H_{wj}(s, t), H_r(t)$  in Eqs. (3.2), (3.3) and (3.5) are defined in the Appendix and the functions  $H_v(s, t), H_w(s, t), H_\phi(s, t)$  are the same as Ref. [24].

The corresponding nondimensional boundary conditions are

$$\begin{aligned}
 v = 0, v' = 0, w = 0, w' = 0 \text{ and} \\
 \phi = 0 \text{ at } s = 0, \tag{3.7}
 \end{aligned}$$

$$\beta_{33} v'' + \beta_{13} \phi' = \varepsilon(B_{v1}(t)) \text{ at } s = 1, \tag{3.8}$$

$$\begin{aligned}
 \beta_{33} v''' + \beta_{13} \phi'' - J_\zeta \ddot{v}' = \varepsilon(B_{v2}(t)) \text{ at} \\
 s = 1, \tag{3.9}
 \end{aligned}$$

$$\beta_{22} w'' = \varepsilon(B_{w1}(t)) \text{ at } s = 1, \tag{3.10}$$

$$\beta_{22} w''' - J_\eta \ddot{w}' = \varepsilon(B_{w2}(t)) \text{ at } s = 1, \tag{3.11}$$

$$\beta_{11} \phi' + \beta_{13} v'' = \varepsilon(B_{\phi1}(t)) \text{ at } s = 1, \tag{3.12}$$

$$r(0) = r_0, \left. \frac{dr}{dt} \right|_{t=0} = 0, \tag{3.13}$$

where the functions  $B_{v1}(t), B_{v2}(t), B_{w1}(t), B_{w2}(t), B_{\phi1}(t)$  are defined in Ref. [24].

### 4 Spatial discretization

The governing Eqs. (3.2)–(3.6) are nonlinear and generally do not have closed-form solution. Since the boundary conditions given in Eqs. (3.7)–(3.13) are spatial and independent of time then the Galerkin method is applied to the equations of motion (3.2)–(3.13) using the following approximation

$$v(s, t) = \phi_v(s) V(t), \tag{4.1}$$

$$w(s, t) = \phi_w(s) W(t), \tag{4.2}$$

$$\phi(s, t) = \phi_\phi(s) E(t), \tag{4.3}$$

In expansions (4.1)–(4.3), the shape functions corresponding to the first mode of a cantilever composite beam without moving mass as used in Ref. [24] have been considered to be replaced into the variables  $v(s, t), w(s, t), \phi(s, t)$ . Multiplying Eqs. (3.2)–(3.4) by weighting functions  $\phi_v(s), \phi_w(s), \phi_\phi(s)$ , respectively, integrating by parts twice, and substituting boundary condition Eqs. (3.7)–(3.13) gives the following semi-discretized equations

$$\begin{aligned}
 (cv_1) \ddot{V} + (cv_2) \dot{V} + (cv_3) V + (cv_4) \\
 E = \varepsilon \left\{ \begin{aligned} & f(E, V, W, \dots) + \frac{1}{2} \left( \int_0^1 \phi_v(s) ds \right) \\ & (f_v \Omega_v^2) (e^{i\Omega_v T_0} + e^{-i\Omega_v T_0}) \end{aligned} \right\}, \tag{4.4}
 \end{aligned}$$

$$\begin{aligned}
 (cw_1) \ddot{W} + (cw_2) \dot{W} + (cw_3) \\
 W = \varepsilon \left\{ \begin{aligned} & g(E, V, W, \dots) + \frac{1}{2} \left( \int_0^1 \phi_w(s) ds \right) \\ & (f_w \Omega_w^2) (e^{i\Omega_w T_0} + e^{-i\Omega_w T_0}) \end{aligned} \right\}, \tag{4.5}
 \end{aligned}$$

$$(c\phi_1) \ddot{E} + (c\phi_2) \dot{E} + (c\phi_3) E + (c\phi_4)$$



$$V = \varepsilon \left\{ h(E, V, W, \dots) + \frac{1}{2} \left( \int_0^1 \phi_\phi(s) ds \right) (f_\phi \Omega_\phi^2) (e^{i\Omega_\phi T_0} + e^{-i\Omega_\phi T_0}) \right\}, \quad (4.6)$$

$$m_s \ddot{r} + k_s r - k_t \dot{q} = \varepsilon k(V, W, \dots) \quad (4.7)$$

$$k_q \ddot{q} + \dot{q} + \varepsilon k_e \dot{r} = 0, \quad (4.8)$$

Coefficients  $cv_i$  ( $i = 1..4$ ),  $cv_{ni}$  ( $i = 1..8$ ),  $cw_i$  ( $i = 1..3$ ),  $cw_{ni}$  ( $i = 1..7$ ) and  $c\phi_i$  ( $i = 1..4$ ),  $c\phi_{ni}$  ( $i = 1..4$ ),  $cr_{ni}$  ( $i = 1..4$ ) in Eqs. (4.4)–(4.7), in addition to coefficients of nonlinear terms, are defined in the Appendix. These coefficients are calculated at the equilibrium position  $s = r_e$  of the moving mass. The power delivered to the electrical circuit due to induction is caused by the magnet mass reciprocating along the beam. The expression for the instantaneous power transferred to the electrical load through the attached coil is derived as

$$P(t) = R_{load} i^2 = R_{load} (\varepsilon k_e \dot{r})^2 \quad (4.9)$$

where the current is obtained from Eq. (4.8) by neglecting the inductance effect relative to the circuit resistance in the  $k_q^*$  expression in Eq. (3.1).

## 5 Solution using the multiple scales method

Equations (4.4)–(4.8) are solved using the method of multiple scales. By defining two time scales  $T_0 = t$  and  $T_1 = \varepsilon t$ , an asymptotic series solution for  $V$ ,  $W$ ,  $E$  and  $r$  are assumed as

$$V(t) = V_0(T_0, T_1) + \varepsilon V_1(T_0, T_1), \quad (5.1)$$

$$W(t) = W_0(T_0, T_1) + \varepsilon W_1(T_0, T_1), \quad (5.2)$$

$$E(t) = E_0(T_0, T_1) + \varepsilon E_1(T_0, T_1), \quad (5.3)$$

$$r(t) = r_0(T_0, T_1) + \varepsilon r_1(T_0, T_1), \quad (5.4)$$

$$q(t) = q_0(T_0, T_1) + \varepsilon q_1(T_0, T_1), \quad (5.5)$$

Using Eqs. (5.1)–(5.5), the Eqs. (4.4)–(4.8) are simplified and coefficients of  $\varepsilon^0$  and  $\varepsilon^1$  are set to zero as follows

Order  $\varepsilon^0$ :

$$(cv_1) D_0^2 V_0 + (cv_3) V_0 + (cv_4) E_0 = 0, \quad (5.6)$$

$$(cw_1) D_0^2 W_0 + (cw_3) W_0 = 0 \quad (5.7)$$

$$(c\phi_1) D_0^2 E_0 + (c\phi_3) E_0 + (c\phi_4) V_0 = 0, \quad (5.8)$$

$$m_s D_0^2 r_0 + k_s r_0 - k_t D_0 q_0 = 0, \quad (5.9)$$

$$k_q D_0^2 q_0 + D_0 q_0 = 0, \quad (5.10)$$

Order  $\varepsilon^1$ :

$$\begin{aligned} (cv_1) D_0^2 V_1 + (cv_3) V_1 + (cv_4) E_1 \\ = f_1(V_0, W_0, E_0, r_0, \dots) \\ + \frac{1}{2} \left( \int_0^1 \phi_v(s) ds \right) (f_v \Omega_v^2) (e^{i\Omega_v T_0} + e^{-i\Omega_v T_0}), \end{aligned} \quad (5.11)$$

$$\begin{aligned} (cw_1) D_0^2 W_1 + (cw_3) W_1 = g_1(W_0, V_0, E_0, r_0, \dots) \\ + \frac{1}{2} \left( \int_0^1 \phi_w(s) ds \right) (f_w \Omega_w^2) (e^{i\Omega_w T_0} + e^{-i\Omega_w T_0}), \end{aligned} \quad (5.12)$$

$$\begin{aligned} (c\phi_1) D_0^2 E_1 + (c\phi_3) E_1 + (c\phi_4) V_1 \\ = h_1(E_0, V_0, W_0, \dots) \\ + \frac{1}{2} \left( \int_0^1 \phi_\phi(s) ds \right) (f_\phi \Omega_\phi^2) (e^{i\Omega_\phi T_0} + e^{-i\Omega_\phi T_0}), \end{aligned} \quad (5.13)$$

$$m_s D_0^2 r_1 + k_s r_1 - k_t D_0 q_1 = k_1(V_0, W_0, r_0, q_0, \dots) \quad (5.14)$$

$$k_q D_0^2 q_1 + D_0 q_1 = j_1(q_0, r_0, \dots), \quad (5.15)$$

which right-hand side terms are appended in the appendix.

By neglecting the magnetic induction ( $L_H = 0$  or  $k_q = 0$ ), solutions to Eqs. (5.6) - (5.10) are given by

$$V_0 = A(T_1) e^{i\omega T_0} + \overline{A(T_1)} e^{-i\omega T_0}, \quad (5.16)$$

$$E_0 = B(T_1) e^{i\omega T_0} + \overline{B(T_1)} e^{-i\omega T_0}, \quad (5.17)$$

$$W_0 = C(T_1) e^{i\rho T_0} + \overline{C(T_1)} e^{-i\rho T_0}, \quad (5.18)$$

$$q_0 = F(T_1) + \overline{F(T_1)}, \quad (5.19)$$

$$r_0 = D(T_1) (e^{i\omega_r T_0}) + \overline{D(T_1)} (e^{-i\omega_r T_0}), \quad (5.20)$$

where,  $A(T_1)$ ,  $\overline{A(T_1)}$ ,  $B(T_1)$ ,  $\overline{B(T_1)}$  and  $C(T_1)$ ,  $\overline{C(T_1)}$ ,  $D(T_1)$ ,  $\overline{D(T_1)}$ ,  $F(T_1)$ ,  $\overline{F(T_1)}$  denote general complex variable functions of the higher time scale and their complex conjugates. The parameter  $\omega$  is the natural frequency of the flapwise-torsional mode,  $\rho$  is the natural frequency of the chordwise mode and  $\omega_r$  is the natural frequency of the moving mass. Substituting Eqs. (5.16) and (5.17) in Eqs. (5.5) and (5.8),  $\omega$  is calculated from Eq. (5.21) which ensures the existence of nontrivial solution.

$$\left[ \begin{array}{c} cv_3 - \omega^2 cv_1 cv_4 \\ c\phi_4 c\phi_3 - \omega^2 c\phi_1 \end{array} \right] = 0, \tag{5.21}$$

$$\left[ \begin{array}{cc} cv_3 - \omega^2 cv_1 & cv_4 \\ c\phi_4 & c\phi_3 - \omega^2 c\phi_1 \end{array} \right] \left[ \begin{array}{c} A(T_1) \\ B(T_1) \end{array} \right] = 0, \tag{5.22}$$

Consequently,

$$B(T_1) = mA(T_1),$$

$$m = \frac{cv_3 - \omega^2 cv_1}{-cv_4} = \frac{-c\phi_4}{c\phi_3 - \omega^2 c\phi_1}. \tag{5.23}$$

where  $\rho$  and  $\omega_r$  are evaluated as follows

$$\rho = \left( \frac{cw_3}{cw_1} \right)^{\frac{1}{2}}, \omega_r = \left( \frac{k_s}{m_s} \right)^{\frac{1}{2}} \tag{5.24}$$

Substituting Eqs. (5.16)–(5.20) into the right hand sides of Eqs. (5.11)–(5.15) and substituting  $D_0q_1$  from Eq. (5.15) in to Eq. (5.14), the following equations are obtained

$$(cv_1)D_0^2V_1 + (cv_3)V_1 + (cv_4)E_1 = \hat{H}_v(T_1)e^{i\omega T_0} + cc + NST, \tag{5.25}$$

$$(cw_1)D_0^2W_1 + (cw_3)W_1 = \hat{H}_w(T_1)e^{i\rho T_0} + cc + NST, \tag{5.26}$$

$$(c\phi_1)D_0^2E_1 + (c\phi_3)E_1 + (c\phi_4)V_1 = \hat{H}_\phi(T_1)e^{i\omega T_0} + cc + NST, \tag{5.27}$$

$$m_s D_0^2 r_1 + k_s r_1 = \hat{H}_r(T_1)e^{i\omega_r T_0} + cc + NST, \tag{5.28}$$

where  $NST$  and  $cc$  stand for the nonsecular and complex conjugate of the preceding terms, respectively. Functions  $\hat{H}_v$ ,  $\hat{H}_w$ ,  $\hat{H}_\phi$  and  $\hat{H}_r$  are secular terms. These terms are determined by assumptions which are considered for internal and external resonances. To eliminate

the secular terms, the coefficients  $\hat{H}_v$ ,  $\hat{H}_w$ ,  $\hat{H}_\phi$  and  $\hat{H}_r$  are set to zero resulting in:

$$\hat{H}_v = 0, \hat{H}_w = 0, \hat{H}_\phi = 0, \hat{H}_r = 0. \tag{5.29}$$

It is essential to mention that the nonlinearity inherent in the present system will permit the establishment of the coupling between flapping and axial modes of vibrations, despite their independence from each other in the linear regime, as seen in Eqs. (5.6)–(5.10).

### 6 Modulation equations

Modulation equations governing the dynamics of interacting modes are obtained from Eq. (5.29) for a graphite-epoxy composite beam with lay-up  $[10_6^0/45_4^0/90_5^0]_s$  which was also considered by Pai [22,23] and Arafat [24]. The properties of the beam are indicated in Table 1. In what follows, we derived the modulation equations for two special cases. In the first case, equations are verified with the equations of the simple composite beam investigated in Refs. [23] and [24] by eliminating the moving mass terms. The second case is considered for the composite beam with a moving mass under flapwise and chordwise base excitation. Hence,

(i) Flapwise excitation without moving mass

In order to verify the modulation equations for a composite beam without moving mass, the same shape functions described in Sect. 4 are employed. From the first natural frequency of the beam and Eq. (5.22), the parameter will be found as  $m = 1$ .

**Table 1** Beam properties

Beam length	$l=1.5\text{ ft}$	Density	$\rho_0 = 96.1\text{ lbm/ft}^3$
Width	$b = 0.37526\text{ in}$	Poisson's ratios	$\nu_{12} = \nu_{13} = 0.24$ $\nu_{23} = 0.49$
Thickness	$h = 0.15\text{ in}$		
Lamina thickness	$h_k = 0.005\text{ in}$	Nondimensional mass moments of inertia	$j_\xi = 5.78704 \times 10^{-6}$ $j_\eta = 3.62192 \times 10^{-5}$ $j_\xi = 4.20062 \times 10^{-5}$
Damping coefficients	$c_v = 0.07, c_w = 0.13, c_\phi = 0.0003$		
Bending and torsional rigidities	$D_{11} = 436.23\text{ lbf.in}^2$ $D_{22} = 5547.2\text{ lbf.in}^2$ $D_{33} = 1532.4\text{ lbf.in}^2$ $D_{13} = 252.02\text{ lbf.in}^2$	Elastic and shear modulus	$E_1 = 1.92 \times 10^7\text{ psi}$ $E_2 = E_3 = 1.56 \times 10^6\text{ psi}$ $G_{23} = 5.23 \times 10^5\text{ psi}$ $G_{13} = G_{13} = 8.20 \times 10^5\text{ psi}$

**Table 2** coefficients of Eqs. (5.20)–(5.22) and natural frequencies

Present study		Ref. [17]	
$\omega = 3.34465975$	$\rho = 6.68905$	$\omega = 3.34465987$	$\rho = 6.68906$
$\Gamma_1 = -1.000043$	$\Lambda_1 = -1.00008$	$\Gamma_1 = -1.00005$	$\Lambda_1 = -1.00008$
$\Gamma_2 = 0.035231$	$\Lambda_2 = 0.064994$	$\Gamma_2 = 0.035232$	$\Lambda_2 = 0.064994$
$\Gamma_3 = -41.37863$	$\Lambda_3 = -20.68937$	$\Gamma_3 = -41.37849$	$\Lambda_3 = -20.68924$
$\Gamma_4 = -20.78856$	$\Lambda_4 = -20.789006$	$\Gamma_4 = -20.78901$	$\Lambda_4 = -20.78901$
$\Gamma_5 = -39.00016$	$\Lambda_5 = -9.27943$	$\Gamma_5 = -39.00110$	$\Lambda_5 = -9.28130$
$\Gamma_6 = -0.39148 f_v \Omega_v^2$		$\Gamma_6 = -0.39149 f_v \Omega_v^2$	

By substituting into Eq. (5.29), we get

$$\hat{H}_v + \hat{H}_\phi = 0, \hat{H}_w = 0, \quad (6.1)$$

$$2i\omega(\Gamma_1)A' = 2i\omega\Gamma_2A - \Gamma_3\bar{A}C e^{2i\omega\delta T_1} - 2\Gamma_4AC\bar{C} - 3\Gamma_5A^2\bar{A} - \Gamma_6 e^{i\omega\sigma T_1}, \quad (6.2)$$

$$2i\rho(\Lambda_1)C' = 2i\rho\Lambda_2C - \Lambda_3A^2 e^{-2i\omega\delta T_1} - 2\Lambda_4A\bar{A}C - 3\Lambda_5C^2\bar{C}, \quad (6.3)$$

where, the coefficients  $\Gamma_i$  ( $i = 1..6$ ) and  $\Lambda_i$  ( $i = 1..5$ ) are defined in the Appendix. For the special case, when  $m_s = 0$  coefficients of modulation equations and natural frequencies are compared to those obtained by Ref. [24] in Table 2. Results show a good agreement between the numerical findings of the present study with those reported in Ref. [24].

(ii) Flapwise and Chordwise excitation

The clamped end of the beam is excited harmonically along the  $v$  direction (i.e., flapwise excitation) and also along the  $w$  direction (i.e., chordwise excitation). The detuning parameters  $\sigma$  and  $\delta$  are defined for two-to-one and one-to-one internal resonances in the following cases:

$$\text{Flapwise excitation } Q_v = f_v \Omega_v^2 \cos(\Omega_v T_0), \\ Q_u = 0, Q_\phi = 0, Q_w = 0,$$

$$\text{Chordwise excitation } Q_w = f_w \Omega_w^2 \cos(\Omega_w T_0), Q_u = 0, Q_\phi = 0, Q_v = 0, \quad (6.4)$$

$$\text{case 1 } \Omega_v = \omega(1 + \varepsilon\sigma), \quad \omega_r = 2\omega(1 + \varepsilon\delta), \\ \text{case 2 } \Omega_w = \rho(1 + \varepsilon\sigma), \quad \omega_r = 2\rho(1 + \varepsilon\delta), \quad (6.5)$$

$$\text{case 3 } \Omega_v = \omega(1 + \varepsilon\sigma), \quad \omega_r = \omega(1 + \varepsilon\delta), \\ \text{case 4 } \Omega_w = \rho(1 + \varepsilon\sigma), \quad \omega_r = \rho(1 + \varepsilon\delta), \quad (6.6)$$

Substituting Eqs. (6.4)–(6.6) into Eq. (5.29) and using Eq. (6.1), we obtain

$$2i\omega(\Gamma_1)A' = 2i\omega\Gamma_2A - 2\Gamma_3AD\bar{D} - 2\Gamma_4AC\bar{C} - 3\Gamma_5A^2\bar{A} - (\Gamma_6\bar{A}D^2 e^{2i\omega\delta T_1} \underline{\mu}_1 + \Gamma_7\bar{A}D e^{2i\omega\delta T_1} \underline{\mu}_2 + \Gamma_8 e^{i\omega\sigma T_1}) \underline{\mu}_F, \quad (6.7)$$

$$2i\rho(\Lambda_1)C' = 2i\rho\Lambda_2C - 2\Lambda_3CD\bar{D} - 2\Lambda_4A\bar{A}C - 3\Lambda_5C^2\bar{C} - (\Lambda_6D^2\bar{C} e^{2i\rho\delta T_1} \underline{\mu}_1 + \Lambda_7\bar{C}D e^{2i\rho\delta T_1} \underline{\mu}_2 + \Lambda_8 e^{i\rho\sigma T_1}) \underline{\mu}_C, \quad (6.8)$$

$$2i\omega_r(X_1)D' = -2X_2A\bar{A}D - 2X_3DC\bar{C} - (X_4A^2\bar{D} e^{-2i\omega\delta T_1} \underline{\mu}_1 + X_5A^2 e^{-2i\omega\delta T_1} \underline{\mu}_2) \underline{\mu}_F - (X_6\bar{D}C^2 e^{-2i\rho\delta T_1} \underline{\mu}_1 + X_7C^2 e^{-2i\rho\delta T_1} \underline{\mu}_2) \underline{\mu}_C, \quad (6.9)$$

where,  $\mu_1$  and  $\mu_2$  are two tracers identifying the terms associated with the one-to-one internal resonance and two-to-one internal resonance, respectively. The equality  $\mu_1 = 1$  implies  $\mu_2 = 0$ , and vice-versa,  $\mu_2 = 1$  requires that  $\mu_1 = 0$ . When  $\mu_1 = \mu_2 = 0$ , there is no internal resonance. Also,  $\mu_F$  and  $\mu_C$  are two tracers associated with flapwise and chordwise excitation terms such that for flapwise excitation  $\mu_F = 1, \mu_C = 0$  and for chordwise excitation  $\mu_F = 0, \mu_C = 1$ .  $\Gamma_i$  ( $i = 1..8$ ),  $\Lambda_i$  ( $i = 1..8$ ),  $X_i$  ( $i = 1..7$ ) are defined in the Appendix.

Complex variables  $A, C, D$  in Eqs. (6.7)–(6.9) are converted to polar form using the following equations

$$\begin{aligned}
 A(T_1) &= \frac{1}{2}a_1(T_1)e^{i\beta_1(T_1)}, C(T_1) = \frac{1}{2}a_2(T_1)e^{i\beta_2(T_1)}, \\
 D(T_1) &= \frac{1}{2}a_3(T_1)e^{i\beta_3(T_1)}, \tag{6.10}
 \end{aligned}$$

Substituting Eq. (6.10) in the Eqs. (6.7)–(6.9) and after some simplifications, we obtain

$$\begin{aligned}
 a'_1 &= \frac{\Gamma_2}{\Gamma_1}a_1 - \left\{ \frac{\Gamma_6}{8\omega\Gamma_1}a_1a_3^2 \sin(\nu_{1f})\underline{\mu}_1 \right. \\
 &\quad \left. + \frac{\Gamma_7}{4\omega\Gamma_1}a_1a_3 \sin(\nu_{2f})\underline{\mu}_2 + \frac{\Gamma_8}{\omega\Gamma_1} \sin(\nu_f) \right\} \underline{\mu}_F \tag{6.11}
 \end{aligned}$$

$$\begin{aligned}
 (a_1\nu'_f - a_1\omega\sigma)\underline{\mu}_F &= -\frac{\Gamma_3}{4\omega\Gamma_1}a_1a_3^2 - \frac{\Gamma_4}{4\omega\Gamma_1}a_1a_2^2 \\
 &\quad - \frac{3\Gamma_5}{8\omega\Gamma_1}a_1^3 - \left\{ \frac{\Gamma_6}{8\omega\Gamma_1}a_1a_3^2 \cos(\nu_{1f})\underline{\mu}_1 \right. \\
 &\quad \left. + \frac{\Gamma_7}{4\omega\Gamma_1}a_1a_3 \cos(\nu_{2f})\underline{\mu}_2 + \frac{\Gamma_8}{\omega\Gamma_1} \cos(\nu_f) \right\} \underline{\mu}_F \tag{6.12}
 \end{aligned}$$

$$\begin{aligned}
 a'_2 &= \frac{\Lambda_2}{\Lambda_1}a_2 - \left\{ \frac{\Lambda_6}{8\rho\Lambda_1}a_2a_3^2 \sin(\nu_{1c})\underline{\mu}_1 \right. \\
 &\quad \left. + \frac{\Lambda_7}{4\rho\Lambda_1}a_2a_3 \sin(\nu_{2c})\underline{\mu}_2 + \frac{\Lambda_8}{\rho\Lambda_1} \sin(\nu_c) \right\} \underline{\mu}_C \tag{6.13}
 \end{aligned}$$

$$\begin{aligned}
 (a_2\nu'_c - \rho\sigma)\underline{\mu}_C &= -\frac{\Lambda_3}{4\rho\Lambda_1}a_2a_3^2 - \frac{\Lambda_4}{4\rho\Lambda_1}a_2^2a_1 \\
 &\quad - \frac{3\Lambda_5}{8\rho\Lambda_1}a_2^3 - \left\{ \frac{\Lambda_6}{8\rho\Lambda_1}a_2a_3^2 \cos(\nu_{1c})\underline{\mu}_1 \right. \\
 &\quad \left. + \frac{\Lambda_7}{4\rho\Lambda_1}a_2a_3 \cos(\nu_{2c})\underline{\mu}_2 + \frac{\Lambda_8}{\rho\Lambda_1} \cos(\nu_c) \right\} \underline{\mu}_C \tag{6.14}
 \end{aligned}$$

$$\begin{aligned}
 a'_3 &= \left\{ \frac{X_4}{8\omega_r X_1}a_3a_1^2 \sin(\nu_{1f})\underline{\mu}_1 \right. \\
 &\quad \left. + \frac{X_5}{4\omega_r X_1}a_1^2 \sin(\nu_{2f})\underline{\mu}_2 \right\} \underline{\mu}_F \\
 &\quad + \left\{ \frac{X_6}{8\omega_r X_1}a_3a_2^2 \sin(\nu_{1c})\underline{\mu}_1 \right. \\
 &\quad \left. + \frac{X_7}{4\omega_r X_1}a_2^2 \sin(\nu_{2c})\underline{\mu}_2 \right\} \underline{\mu}_C \tag{6.15} \\
 &- a_3 \left\{ \left( \frac{\nu'_{1f}}{2} - \nu'_f + \omega(\sigma - \delta) \right) \underline{\mu}_1 \right. \\
 &\quad \left. + (\nu'_{2f} - 2\nu'_f + 2\omega(\sigma - \delta))\underline{\mu}_2 \right\} \underline{\mu}_F \\
 &- a_3 \left\{ \left( \frac{\nu'_{1c}}{2} - \nu'_c + \rho(\sigma - \delta) \right) \underline{\mu}_1 \right.
 \end{aligned}$$

$$\begin{aligned}
 &\quad \left. + (\nu'_{2c} - 2\nu'_c + 2\rho(\sigma - \delta))\underline{\mu}_2 \right\} \underline{\mu}_C = \frac{-X_2}{4\omega_r X_1}a_1^2a_3 \\
 &\quad - \frac{X_3}{4\omega_r X_1}a_2a_3 - \left\{ \frac{X_4}{8\omega_r X_1}a_1^2a_3 \cos(\nu_{1f})\underline{\mu}_1 \right. \\
 &\quad \left. + \frac{X_5}{4\omega_r X_1}a_1^2 \cos(\nu_{2f})\underline{\mu}_2 \right\} \underline{\mu}_F \\
 &\quad - \left\{ \frac{X_6}{8\omega_r X_1}a_2^2a_3 \cos(\nu_{1c})\underline{\mu}_1 \right. \\
 &\quad \left. + \frac{X_7}{4\omega_r X_1}a_2^2 \cos(\nu_{2c})\underline{\mu}_2 \right\} \underline{\mu}_C, \tag{6.16}
 \end{aligned}$$

where,

$$\begin{aligned}
 \nu_f &= \omega\sigma T_1 - \beta_1, \quad \nu_c = \rho\sigma T_1 - \beta_2, \\
 \nu_{1f} &= 2\beta_3 - 2\beta_1 + 2\omega\delta T_1, \\
 \nu_{2f} &= \beta_3 - 2\beta_1 + 2\omega\delta T_1, \\
 \nu_{1c} &= 2\beta_3 - 2\beta_2 + 2\rho\delta T_1, \\
 \nu_{2c} &= \beta_3 - 2\beta_2 + 2\rho\delta T_1, \tag{6.17}
 \end{aligned}$$

Alternatively, we express the A and C, D in the Cartesian form as

$$\begin{aligned}
 A(T_1) &= \frac{1}{2}(p_1 - iq_1)e^{i\omega\sigma T_1}, C(T_1) \\
 &= \frac{1}{2}(p_2 - iq_2)e^{i\rho\sigma T_1}, \\
 D(T_1) &= \frac{1}{2}(p_3 - iq_3)\{ (e^{i\omega(\sigma-\delta)T_1}\underline{\mu}_1 \\
 &\quad + e^{2i\omega(\sigma-\delta)T_1}\underline{\mu}_2)\underline{\mu}_F + (e^{i\rho(\sigma-\delta)T_1}\underline{\mu}_1 \\
 &\quad + e^{2i\rho(\sigma-\delta)T_1}\underline{\mu}_2)\underline{\mu}_C \}, \tag{6.18}
 \end{aligned}$$

By separating the real and imaginary parts in Eqs. (6.7)–(6.9), one obtain

$$\begin{aligned}
 p'_1 &= -\omega\sigma q_1 + \frac{\Gamma_2}{\Gamma_1}p_1 + \frac{\Gamma_3}{4\omega\Gamma_1}(q_1p_3^2 + q_1q_3^2) \\
 &\quad + \frac{\Gamma_4}{4\omega\Gamma_1}(q_1p_2^2 + q_1q_2^2) \\
 &\quad + \frac{3\Gamma_5}{8\omega\Gamma_1}(q_1p_1^2 + q_1^3) \\
 &\quad + \left\{ \frac{\Gamma_6}{8\omega\Gamma_1}(2p_1p_3q_3 - q_1p_3^2 + q_1q_3^2)\underline{\mu}_1 \right. \\
 &\quad \left. + \frac{\Gamma_7}{4\omega\Gamma_1}(p_1q_3 - q_1p_3)\underline{\mu}_2 \right\} \underline{\mu}_F, \tag{6.19} \\
 q'_1 &= \omega\sigma p_1 + \frac{\Gamma_2}{\Gamma_1}q_1 \\
 &\quad - \frac{\Gamma_3}{4\omega\Gamma_1}(p_1p_3^2 + p_1q_3^2) \\
 &\quad - \frac{\Gamma_4}{4\omega\Gamma_1}(p_1p_2^2 + p_1q_2^2) - \frac{3\Gamma_5}{8\omega\Gamma_1}(p_1q_1^2 + p_1^3)
 \end{aligned}$$

$$\begin{aligned}
& - \left\{ \frac{\Gamma_6}{8\omega\Gamma_1} (2q_1 p_3 q_3 - p_1 q_3^2 + p_1 p_3^2) \underline{\underline{\mu}}_1 \right. \\
& \left. + \frac{\Gamma_7}{4\omega\Gamma_1} (p_1 p_3 + q_1 q_3) \underline{\underline{\mu}}_2 \right\} \underline{\underline{\mu}}_F, \quad (6.20)
\end{aligned}$$

$$\begin{aligned}
p'_2 = & -\rho\sigma q_2 + \frac{\Lambda_2}{\Lambda_1} p_2 + \frac{\Lambda_3}{4\rho\Lambda_1} (q_2 p_3^2 + q_2 q_3^2) \\
& + \frac{\Lambda_4}{4\rho\Lambda_1} (q_2 p_1^2 + q_2 q_1^2) \\
& + \frac{3\Lambda_5}{8\rho\Lambda_1} (q_2 p_2^2 + q_2^3) \\
& + \left\{ \frac{\Lambda_6}{8\rho\Lambda_1} (2p_2 p_3 q_3 - q_2 p_3^2 + q_2 q_3^2) \underline{\underline{\mu}}_1 \right. \\
& \left. + \frac{\Lambda_7}{4\rho\Lambda_1} (p_2 q_3 - q_2 p_3) \underline{\underline{\mu}}_2 \right\} \underline{\underline{\mu}}_c, \quad (6.21)
\end{aligned}$$

$$\begin{aligned}
q'_2 = & \rho\sigma p_2 + \frac{\Lambda_2}{\Lambda_1} q_2 - \frac{\Lambda_3}{4\rho\Lambda_1} (p_2 p_3^2 + p_2 q_3^2) \\
& - \frac{\Lambda_4}{4\rho\Lambda_1} (p_2 p_1^2 + p_2 q_1^2) - \frac{3\Lambda_5}{8\rho\Lambda_1} (p_2 q_2^2 + p_2^3) \\
& - \left\{ \frac{\Lambda_6}{8\rho\Lambda_1} (2q_2 p_3 q_3 - p_2 q_3^2 + p_2 p_3^2) \underline{\underline{\mu}}_1 \right. \\
& \left. + \frac{\Lambda_7}{4\rho\Lambda_1} (p_2 p_3 + q_2 q_3) \underline{\underline{\mu}}_2 + \frac{\Lambda_8}{\rho\Lambda_1} \right\} \underline{\underline{\mu}}_c, \quad (6.22)
\end{aligned}$$

$$\begin{aligned}
p'_3 = & (-\omega(\sigma - \delta) q_3 \underline{\underline{\mu}}_1 - 2\omega(\sigma - \delta) q_3 \underline{\underline{\mu}}_2) \underline{\underline{\mu}}_F \\
& + (-\rho(\sigma - \delta) q_3 \underline{\underline{\mu}}_1 - 2\rho(\sigma - \delta) q_3 \underline{\underline{\mu}}_2) \underline{\underline{\mu}}_c \\
& \frac{X_2}{4\omega_r X_1} (p_1^2 q_3 + q_1^2 q_3) + \frac{X_3}{4\omega_r X_1} (p_2^2 q_3 + q_2^2 q_3) \\
& + \left\{ \frac{X_4}{8\omega_r X_1} (q_1^2 q_3 + 2p_1 q_1 p_3 - p_1^2 q_3) \underline{\underline{\mu}}_1 \right. \\
& \left. + \frac{X_5}{2\omega_r X_1} p_1 q_1 \underline{\underline{\mu}}_2 \right\} \underline{\underline{\mu}}_F \\
& + \left\{ \frac{X_6}{8\omega_r X_1} (2p_2 q_2 p_3 - q_3 p_2^2 + q_2^2 q_3) \underline{\underline{\mu}}_1 \right. \\
& \left. + \frac{X_7}{2\omega_r X_1} (p_2 q_2) \underline{\underline{\mu}}_2 \right\} \underline{\underline{\mu}}_c, \quad (6.23)
\end{aligned}$$

$$\begin{aligned}
q'_3 = & (\omega(\sigma - \delta) p_3 \underline{\underline{\mu}}_1 + 2\omega(\sigma - \delta) p_3 \underline{\underline{\mu}}_2) \underline{\underline{\mu}}_F \\
& + (\rho(\sigma - \delta) p_3 \underline{\underline{\mu}}_1 + 2\rho(\sigma - \delta) p_3 \underline{\underline{\mu}}_2) \underline{\underline{\mu}}_c \\
& - \frac{X_2}{4\omega_r X_1} (q_1^2 p_3 + p_1^2 p_3) \\
& - \frac{X_3}{4\omega_r X_1} (p_2^2 p_3 + q_2^2 p_3) \\
& - \left\{ \frac{X_4}{8\omega_r X_1} (p_1^2 p_3 - q_1^2 p_3 + 2p_1 q_1 q_3) \underline{\underline{\mu}}_1 \right.
\end{aligned}$$

$$\begin{aligned}
& \left. + \frac{X_5}{4\omega_r X_1} (p_1^2 - q_1^2) \underline{\underline{\mu}}_2 \right\} \underline{\underline{\mu}}_F \\
& - \left\{ \frac{X_6}{8\omega_r X_1} (p_3 p_2^2 + 2p_2 q_2 q_3 - q_2^2 p_3) \underline{\underline{\mu}}_1 \right. \\
& \left. + \frac{X_7}{4\omega_r X_1} (p_2^2 - q_2^2) \underline{\underline{\mu}}_2 \right\} \underline{\underline{\mu}}_c, \quad (6.24)
\end{aligned}$$

The fixed points of Eqs. (6.11)–(6.16) correspond to  $a'_1 = a'_2 = a'_3 = v'_f = v'_c = v'_{1f} = v'_{1c} = v'_{2f} = v'_{2c} = 0$  or  $p'_1 = q'_1 = p'_2 = q'_2 = p'_3 = q'_3 = 0$  for various cases. A pseudo arc length scheme is used to trace branches of equilibrium solutions and fixed points may lose stability due to saddle-point bifurcations or Hopf bifurcations. Then, the amplitudes  $a_1$ ,  $a_2$  and  $a_3$  are calculated from  $a_i = \sqrt{p_i^2 + q_i^2}$ . The stability of a fixed point is ascertained by investigating eigenvalues of the Jacobian matrix of the right-hand sides of Eqs. (6.19)–(6.24).

As it concerns the efficiency of this harvesting device, some approximate calculations permit to give an evaluation as follows. For the flapwise excitation case, the input power is derived by calculating the average work done of the base excitation force in the flapwise direction over one time period:

$$\begin{aligned}
P_i = & \frac{1}{(2\pi/\Omega)} = \int_0^{2\pi/\Omega} \int_0^\ell Q_{v,v}(x,t) dx dt = \frac{\Omega}{2\pi} \\
& = \int_0^{2\pi/\Omega} \int_0^\ell f_v \Omega^2 \cos(\Omega t) a_1(T_1) \\
& \quad \times \cos(\omega T_0 + \beta_1(T_1)) \varphi_v(x) dx dt \\
& = a_1 f_v \Omega^2 \left( \int_0^\ell \varphi_v(x) dx \right) \cos \beta_1 \quad (6.25)
\end{aligned}$$

The average power delivered to the electrical circuit is due to induction of the reciprocating magnet mass along the beam. The expression for the average power transferred to the electrical load through the attached coil is derived as

$$\begin{aligned}
P_o = & \frac{\Omega}{2\pi} = \int_0^{2\pi/\Omega} R_{load} i^2 dt = \frac{\Omega}{2\pi} = \int_0^{2\pi/\Omega} R_{load} (\varepsilon k_e \dot{r})^2 dt \\
& = \frac{\Omega}{2\pi} R_{load} \varepsilon k_e^2 \int_0^{2\pi/\Omega} [-a_3(T_1) \omega_r \sin(\omega_r T_0 \\
& \quad + \beta_3(T_1))]^2 dt = 2 R_{load} \varepsilon^2 k_e^2 a_3^2 \Omega^2 \quad (6.26)
\end{aligned}$$

Subsequently one can calculate the power transfer efficiency as:

$$\eta \triangleq \frac{P_o}{P_i} = \frac{2R_{load}\varepsilon^2k_e^2}{\left(\int_0^\ell \varphi_v(x)dx\right) \cos \beta_1} \cdot \frac{1}{f_v} \cdot \frac{a_3^2}{a_1} \propto \frac{1}{f_v} \cdot \frac{a_3^2}{a_1} \tag{6.27}$$

This latter relationship shows how the efficiency may vary with excitation force. Next through simulations, enhancement of harvester efficiency while entering the nonlinear domain will be demonstrated.

### 7 Results

The steady-state behavior of the composite beam carrying a moving mass is investigated under flapwise and chordwise excitation. The mass ratio and equilibrium position of the moving mass with respect to the beam are, respectively, set to 0.05 and 0.5. Natural frequencies corresponding to flapwise-torsional and chordwise modes are obtained as  $\omega = 3.40293157$ ,  $\rho = 6.6132826$ , respectively. Desirable quantities for the oscillator parameters are determined accordingly to reproduce the one-to-one and two-to-one internal resonances conditions in flapwise and chordwise excitations. Resulting steady-state solutions are presented through frequency-response and force-response diagrams. In all figures, solid lines indicate stable solutions, dashed lines indicate unstable solutions with at

least one eigenvalue being positive and the dotted lines indicate the unstable solutions with the real part of a complex conjugate pair of eigenvalues being positive.

#### 7.1 Flapwise excitation result

Results presented in this section are related to the flapwise excitation in Eq. (6.4) and the cases 1 and 3 in Eqs. (6.5)–(6.6) with the force amplitude  $f_v = 0.01$  in flapwise direction. The chordwise direction can also be excited alongside the flapwise excitation by a force of amplitude  $f_w \neq 0$ , assuming that external resonance in this direction is not activated. Dimensionless values of spring stiffness necessary for generating one-to-one and two-to-one internal resonance are evaluated as  $k_s = 0.578997$  and  $k_s = 2.3160$ , respectively. The numerical values of parameters proposed in Ref.[16], namely  $R_{int} = 188\Omega$ ,  $R_{load} = 1 \times 10^6\Omega$ ,  $\alpha = 7.752Vs/m$ , are selected for the simulations. The coil turns per unit length and coil radius are  $n = 200$ ,  $R_c = 0.4in$ , respectively.

Figure 3a, b show force–response curves of the one-to-one internal resonance condition for internal and external detuning parameters  $\delta = 0.01$ ,  $\sigma = 0$ . As shown in Fig. 3a, b, the input energy is transferred from the flapwise-torsional mode to the moving mass at  $f_{v1} = 0.00315$  through a saddle-node bifurcation and this mode saturates to a constant value  $a_1$ . As  $f_v$  increases from zero, the  $a_1$  amplitude reverses from point A at  $f_{v1} = 0.00315$  to point B at  $f_{v2}=0.00234$

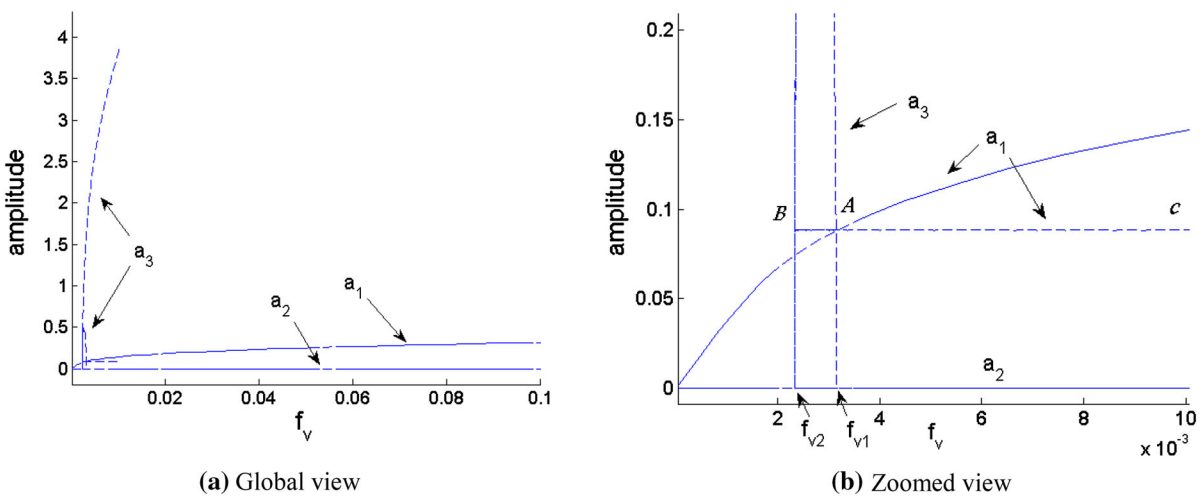
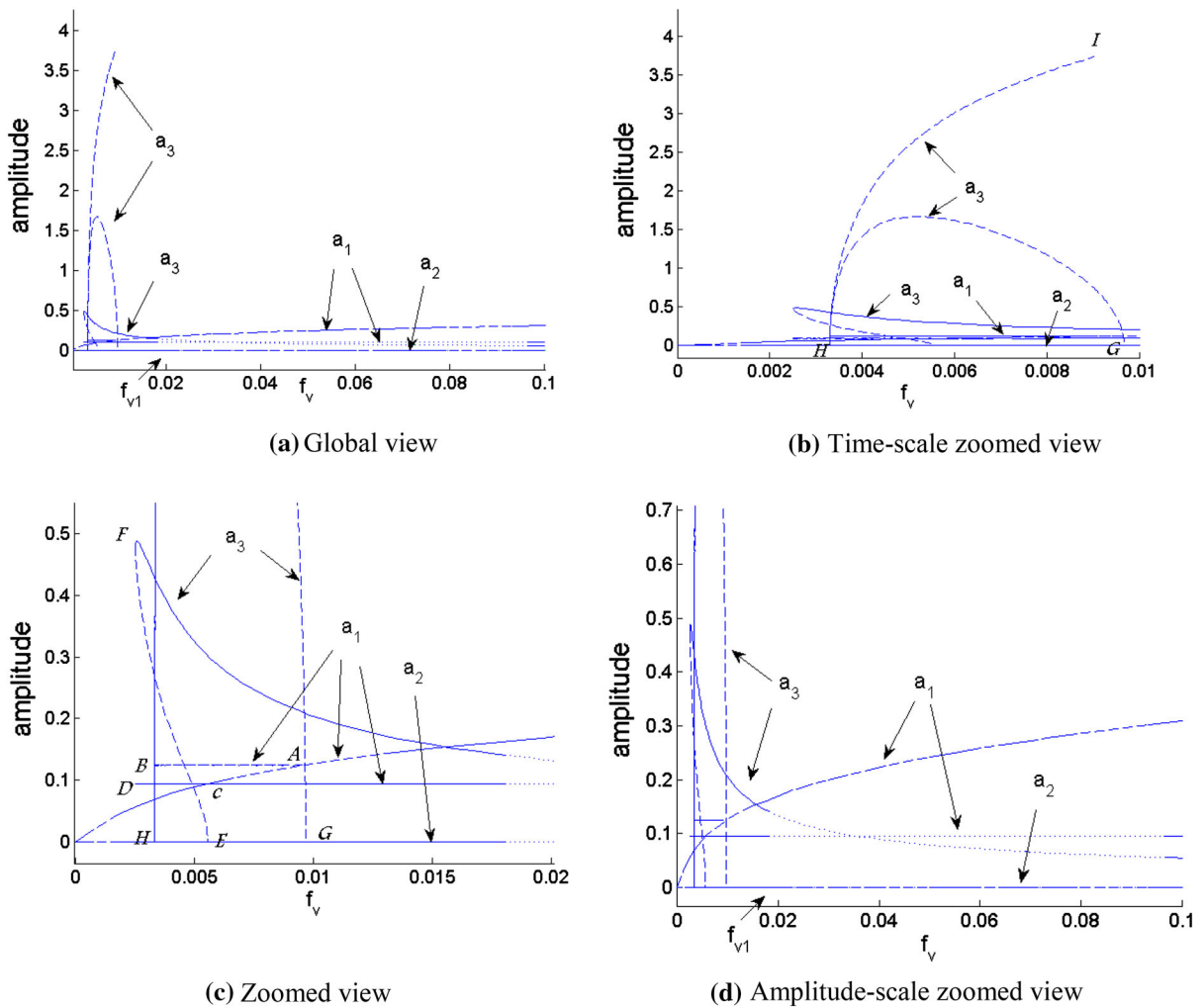


Fig. 3 Force–response curves for one-to-one internal resonance and parameters  $\delta = 0.01$ ,  $\sigma = 0$



**Fig. 4** Force–response curves for one-to-one internal resonance and parameters  $\delta = 0.01$ ,  $\sigma = -0.01$

as shown in Fig. 3b and the  $a_3$  amplitude traces unstable solution  $DE$  as shown in Fig. 3b. Figure 4 shows force–response curves for detuning parameters  $\delta = 0.01$ ,  $\sigma = -0.01$ . Saturation of flapwise-torsional mode is shown in this figure as  $f_v$  is increased from zero to 0.1. As shown in Fig. 4a, d, fixed points lose their stability through a Hopf bifurcation at  $f_{v1} = 0.0181$  resulting in the creation of limit cycles for amplitudes and phases. The response curves in parts (b) and (c) undergo subcritical pitchfork bifurcations at points  $E$  and  $G$ . Furthermore, there is an interval of the force amplitude  $f_v$  after  $f_{v1}$  in Fig. 4d in which no stable fixed point exists. Hence, the response of the beam in this interval is expected to be aperiodic including chaotic. In order to verify the claim, phase

plane evolutions of the involved variables have been depicted, although not necessarily chaotic but presenting complex aperiodic behaviors for  $\delta = 0.01$ ,  $\sigma = -0.01$ ,  $f_v = 0.03$  as shown in Fig. 5, and is completely periodic for  $\delta = 0.01$ ,  $\sigma = -0.01$ ,  $f_v = 0.02$  as shown in Fig. 6. The behavior of these operational points is found out as predicted with perturbation method.

Frequency-response of composite beam carrying a moving mass is shown in Fig. 7a, b for  $\delta = 0.01$  and  $\delta = -0.01$ , respectively. Saddle-node bifurcation occurs at  $\sigma = -0.0103$  for  $\delta = 0.01$  and at  $\sigma = -0.0238$  for  $\delta = -0.01$ . In Fig. 7, a region of frequency detuning  $\sigma$  appears in which no stable fixed point exists.

The steady-state behavior of the composite beam carrying a moving mass is investigated in the two-to-

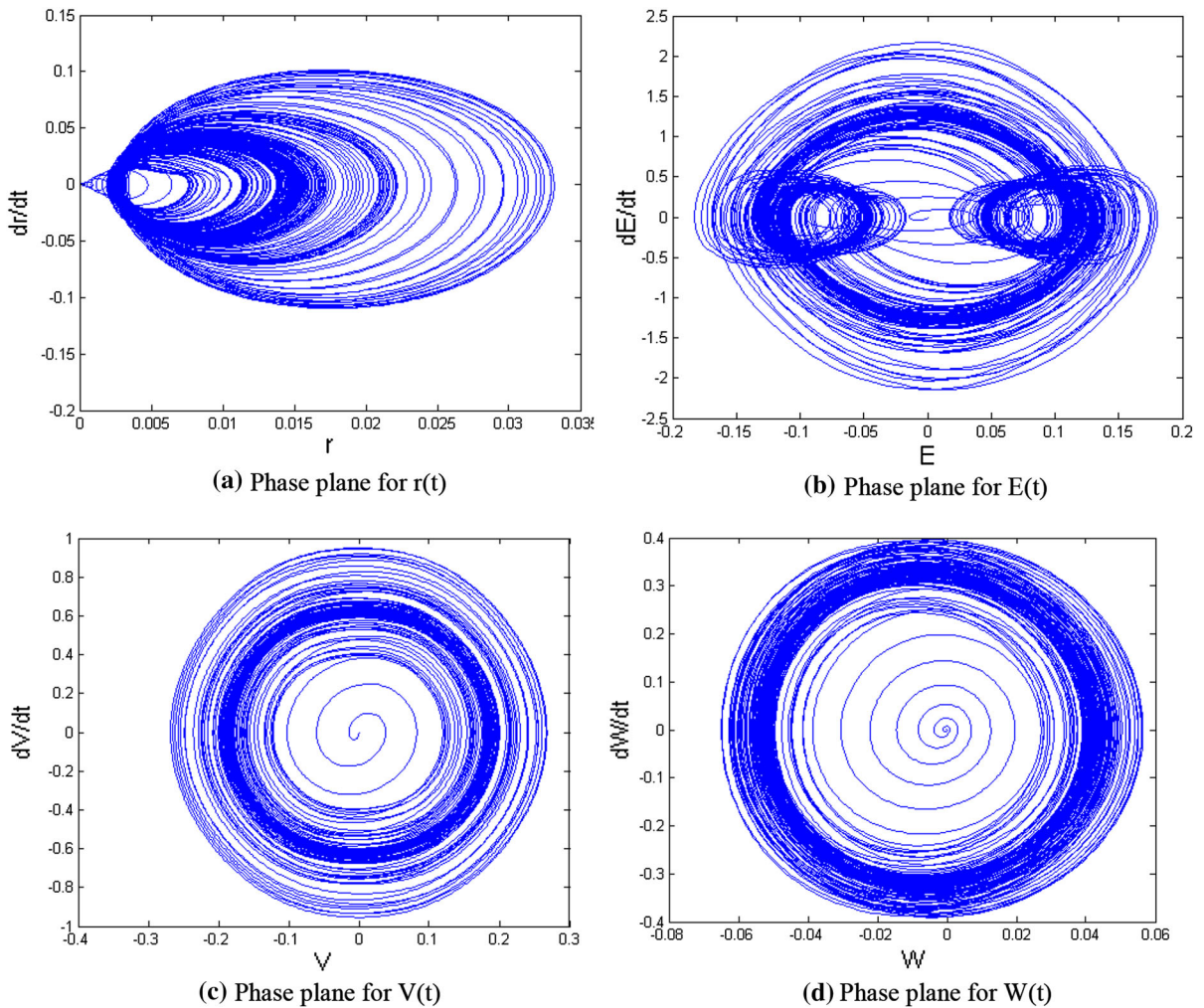


**Fig. 5** Phase plane response two-to-one internal resonance and  $\delta = 0.01$ ,  $\sigma = -0.01$ ,  $f_v = 0.03$

one internal resonance condition. Figure 8a, b show the force–response curves when  $\delta = 0.01$ ,  $\sigma = 0$ . The directly excited mode ( $a_1$  amplitude) saturates to a constant value equal to 0.15 and the input energy is transferred to the moving mass.

Figures 9 and 10 show the numerical integration for two points A and B presented in Fig. 8a. In these figures,  $V(t)$ ,  $E(t)$ ,  $W(t)$ ,  $r(t)$  are plotted versus time for the system evaluated at operational points A and B. It is seen that the response amplitude is very close to the value predicted by the perturbation method. Figures 9c and 10a show that the saturation of flapwise mode (mode  $a_2$ ) is promoted in numerical solutions.

In order to confirm the output characteristics of the results, the frequency content of the time signals is

obtained by taking their fast Fourier transform. Taking into account Nyquist-Shannon theorem, frequency spectrum  $V(f)$ ,  $E(f)$  and  $r(f)$ ,  $W(f)$  have been sketched in Fig. 9 in adjacency to their corresponding time histories, corresponding to operational point A of Fig. 8a. As shown, in the spectrum peaks appear near first-mode frequencies and the two-to-one internal resonance condition ( $\omega = 3.4$ ,  $\omega_r = 6.8$ ) is confirmed. Moreover, flapping response amplitude remains constant with respect to force amplitude modulation as presented in Figs. 9c, 10a, corresponding, respectively, to point A and B in Fig. 8a. As shown, amplitude and frequencies of the oscillations obtained numerically compared well with indicated values resulted from the semi-analytic perturbation method.



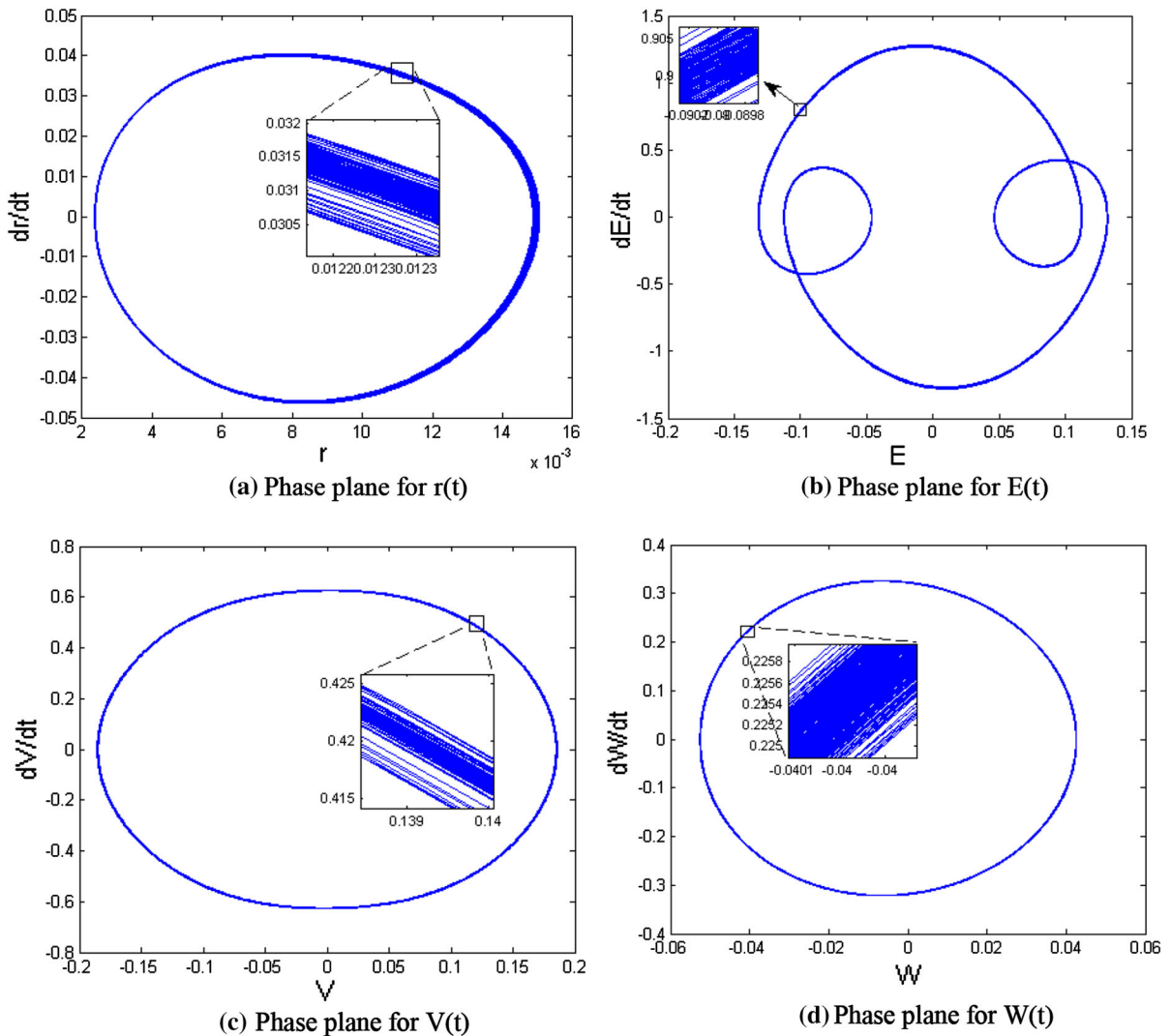


**Fig. 6** Phase plane response two-to-one internal resonance and  $\delta = 0.01$ ,  $\sigma = -0.01$ ,  $f_v = 0.02$

By referring to Fig. 8 which indicates the vibration amplitudes modulation against base excitation magnitude, it is seen that slightly increasing base force  $f_v$  causes a multi-fold magnification of  $a_3$  amplitude while  $a_1$  amplitude saturates to a constant value, thus enhancing the harvester efficiency according to relationship Eq. (6.27). This demonstrates that harvester efficiency improves as it is progressing further in the nonlinear domain.

Figures 11a and b, display force–response when  $\delta = 0.01$ ,  $\sigma = -0.01$  and the system exhibits saturation phenomenon for the directly excited mode. Figure 12 shows frequency–response curves when  $\delta =$

$0.01, -0.01, 0.05, -0.11$ . As shown in Fig. 12a–c, when  $\sigma$  is increased, we have a single mode solution, which is stable, and fixed points experience a saddle-node bifurcation at  $\sigma = -0.00428$ ,  $\sigma = -0.0198$ ,  $\sigma = -0.0255$ , respectively. In Fig. 12d, the plant exhibits a hardening-type behavior which leads to a jump dynamic solution.

## 7.2 Chordwise excitation result

Results presented in this section are related to the chordwise excitation in Eq. (6.4) and the cases 2 and 4 in Eqs. (6.5)–(6.6) and for the force ampli-

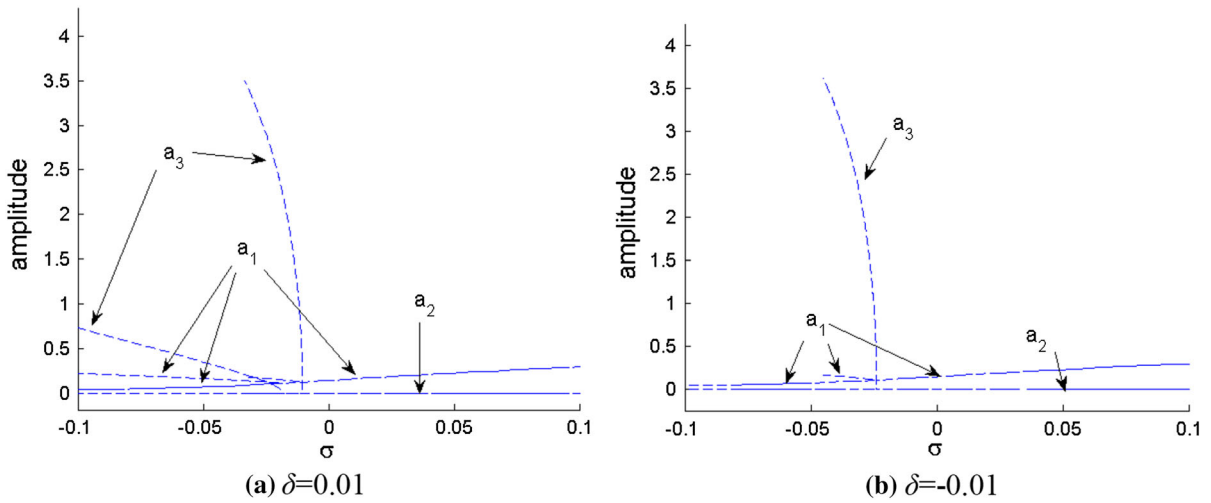


Fig. 7 Frequency-response curves for one-to-one internal resonance

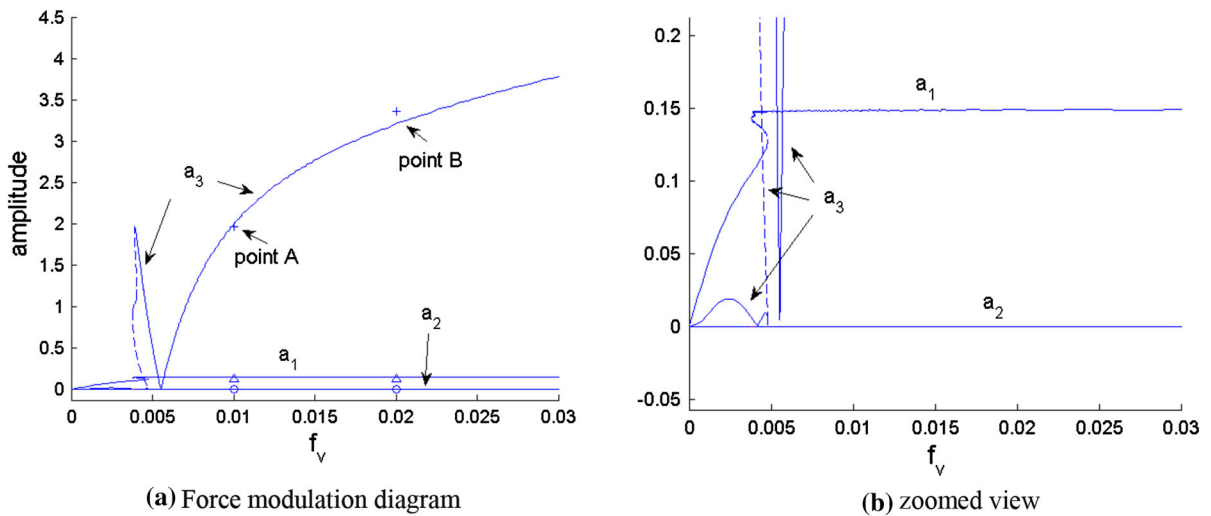
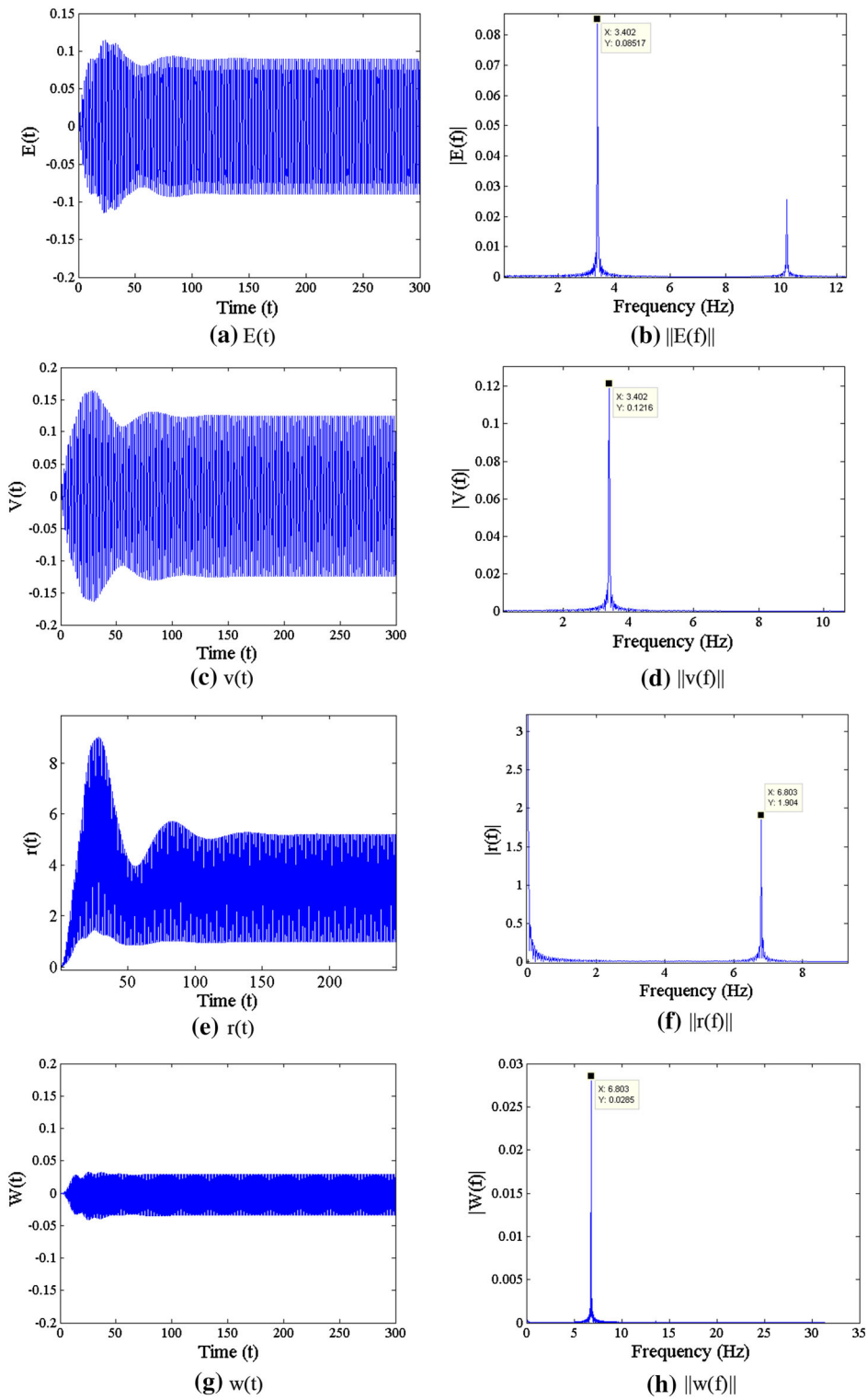


Fig. 8 Force-response curves for two-to-one internal resonance and  $\delta = 0.01, \sigma = 0$

tude in chordwise direction  $f_w = 0.01$ . Flapwise direction can still be excited simultaneously with chordwise excitation,  $f_v \neq 0$ , if resonance in this direction is not approached. Dimensionless values of spring stiffness for establishing one-to-one and two-to-one internal resonance are evaluated as  $k_s = 2.1867753$  and  $k_s = 8.7471$ , respectively. The coil parameters are the same as those selected for flapwise excitation.

In Fig. 13, the force-response curve is shown for one-to-one internal resonance when  $\delta = 0.01$  and  $\sigma = 0, -0.01$ . As shown in Fig. 13a, as  $f_w$  is increased from

zero, the directly excited mode ( $a_2$  amplitude) linearly increases and the solution undergoes a Hopf bifurcation at  $f_{w1} = 0.00203$ , leading to a two-mode dynamic solution for  $a_2$  and  $a_3$  amplitudes. When  $f > f_{w1}$ , depending on the amplitude of the motion, the response may be attracted to either a dynamic or a constant solution. In this case, the plant's amplitude may saturate at value  $a_2$ . Figure 13b shows force-response curve for  $\delta = 0.01$  and  $\sigma = -0.01$ . Fixed points lose stability through a Hopf bifurcation at  $f_{w1} = 0.00289$ . Also, saturation of the directly excited mode is presented in this figure.



**Fig. 9** Time-response curves of vibration amplitude ( $V, W, E, r$ ) corresponding to operational point A of Fig. 8a with their corresponding FFTs

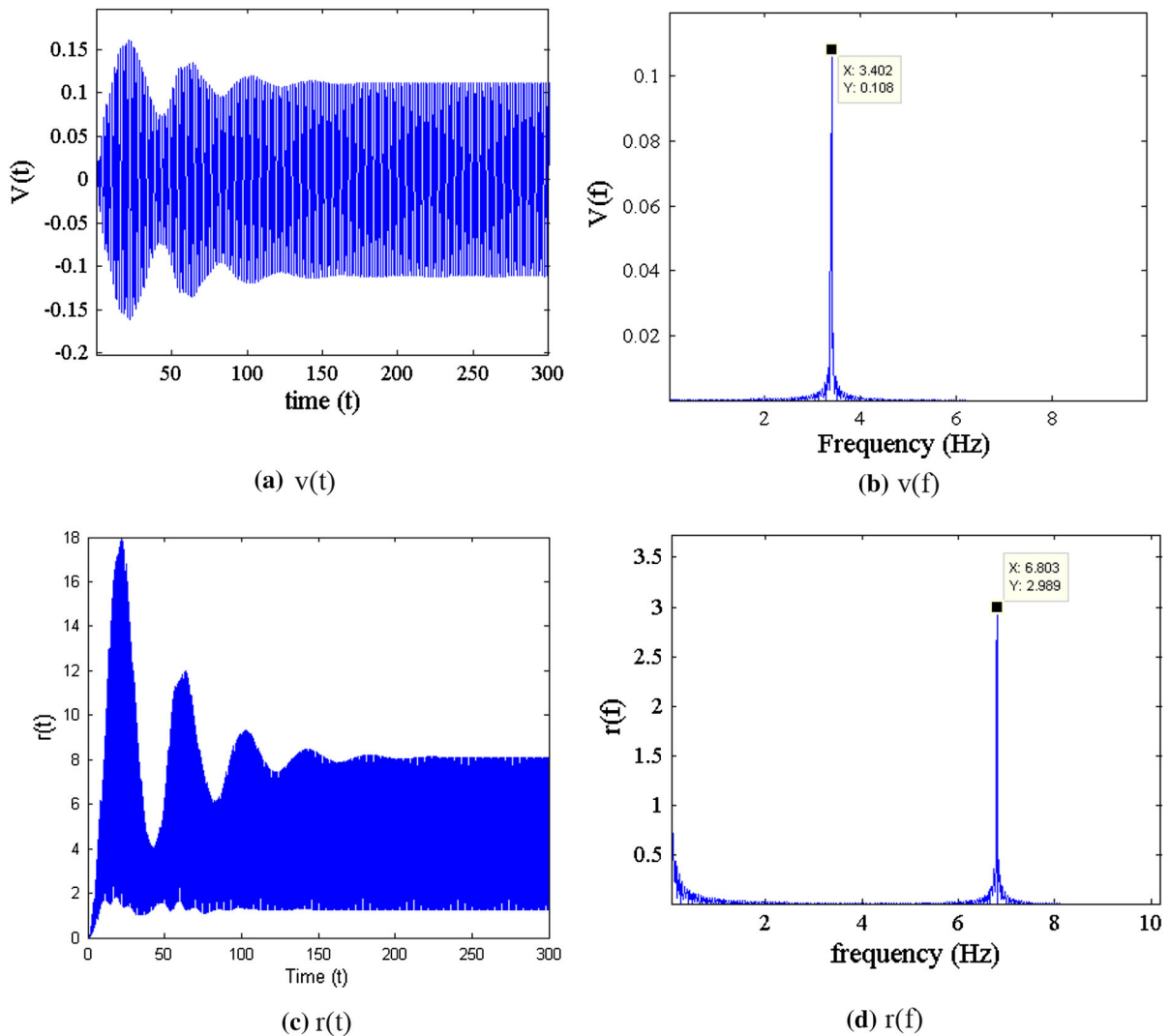
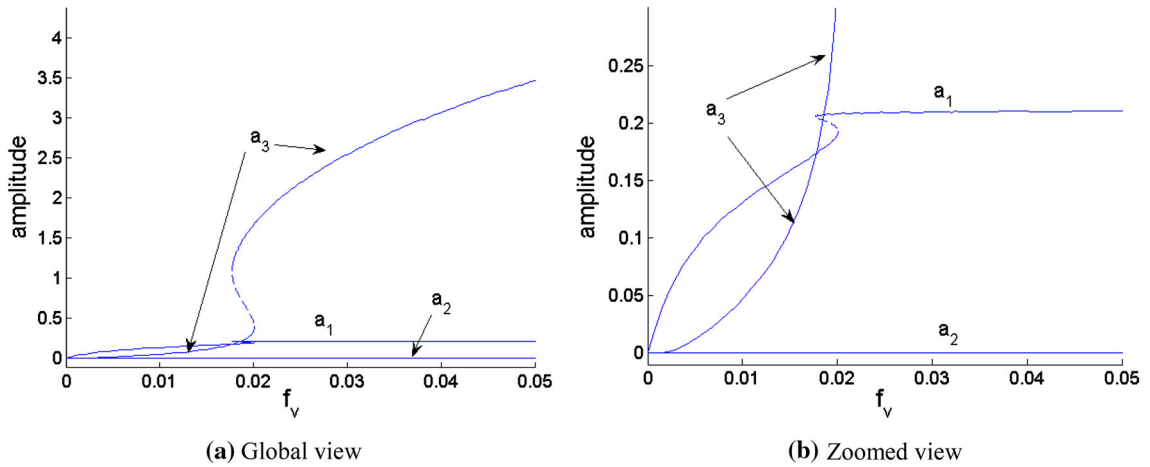


**Fig. 10** Time-response curves of vibration amplitude ( $V$ ,  $r$ ) corresponding to operational point B of Fig. 8a with their corresponding FFTs

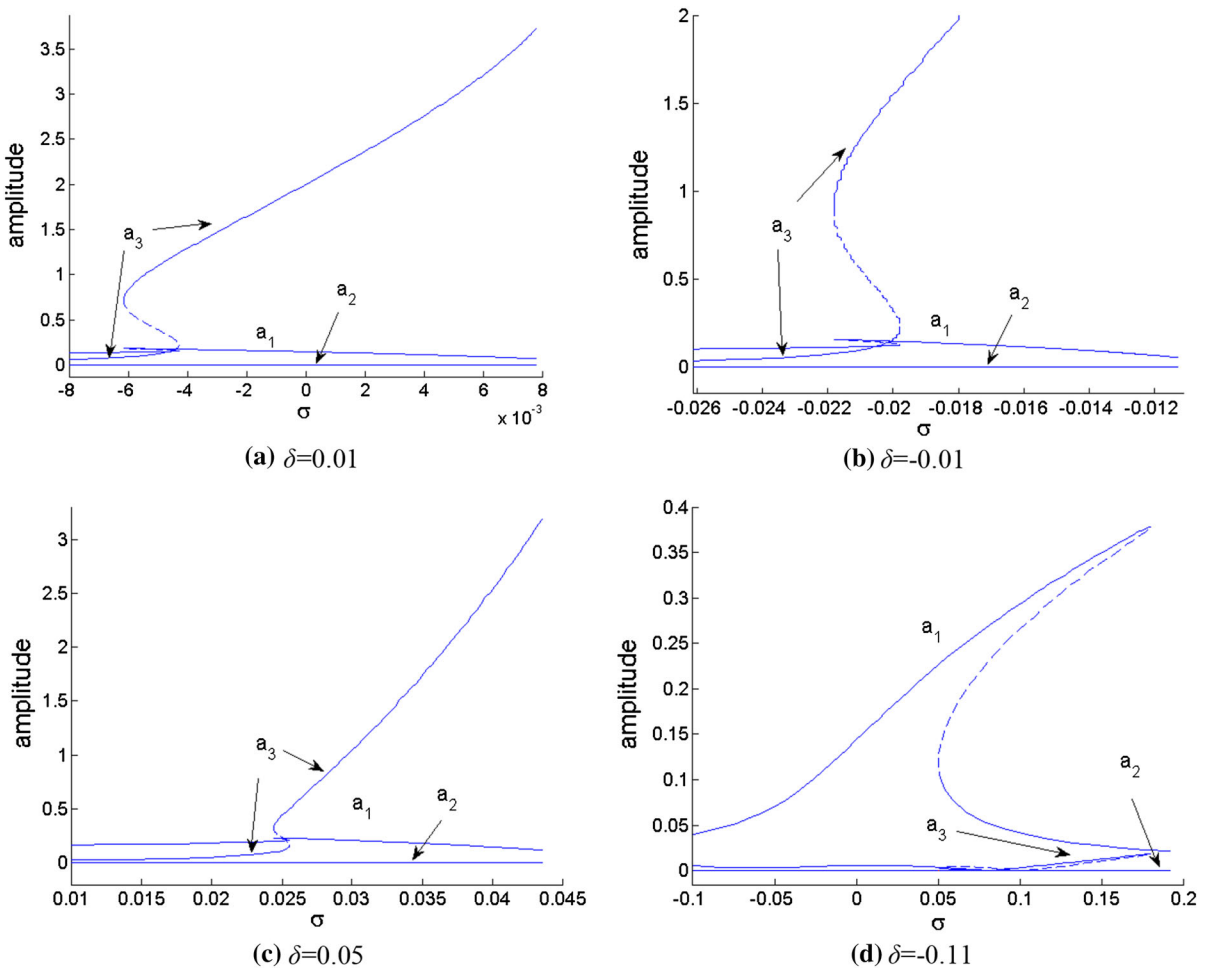
Figure 14 shows frequency-response curves for one-to-one internal resonance when  $\delta = 0.01$  and  $\delta = -0.01$ . As shown in Fig. 14a, a Hopf bifurcation occurs at  $\sigma = \sigma_1 = -0.0277$  which leads to two branch solutions for  $a_2$  and  $a_3$  amplitudes. Figure 14b shows the amplitude of unstable solution of moving mass or  $a_3$  amplitude. The response goes through a saddle-node bifurcation which leads to a jump phenomenon in the system. Figure 14c, d show the frequency-response curves when  $\delta = -0.01$ . Stable and unstable fixed points correspond to saddle-node bifurcation.

Figure 15a, b are produced for two-to-one internal resonance case when  $\delta = -0.01$ . These figures show force-response curves for  $\delta = -0.01$ ,  $\sigma = 0$  and  $\delta = -0.01$ ,  $\sigma = 0.01$ , respectively. The response consists of the single-mode unstable solution. As  $f$  is increased from zero, the directly excited mode saturates and the unexcited mode ( $a_3$  amplitude) increases.

Figure 16 shows frequency-response curves for two-to-one internal resonance when  $\delta = 0.01, -0.01, 0.05, 0.11$ . As shown in Fig. 16a–d, the response consists of unstable solutions.



**Fig. 11** Force–response curves for two-to-one internal resonance and  $\delta = 0.01, \sigma = -0.01$



**Fig. 12** Frequency–response curves for two-to-one internal resonance

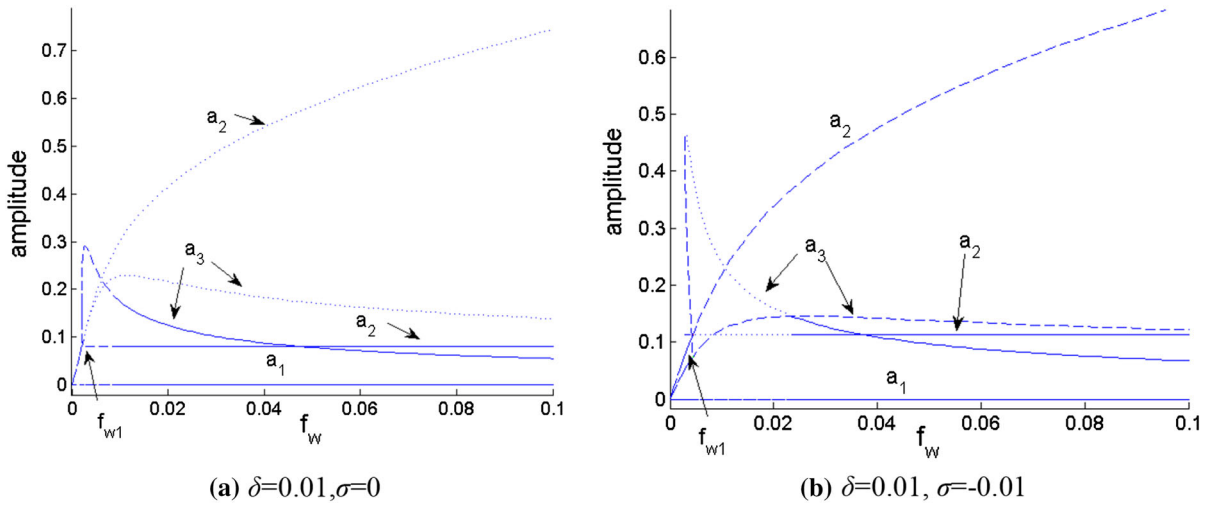


Fig. 13 Force-response curves for one-to-one internal resonance

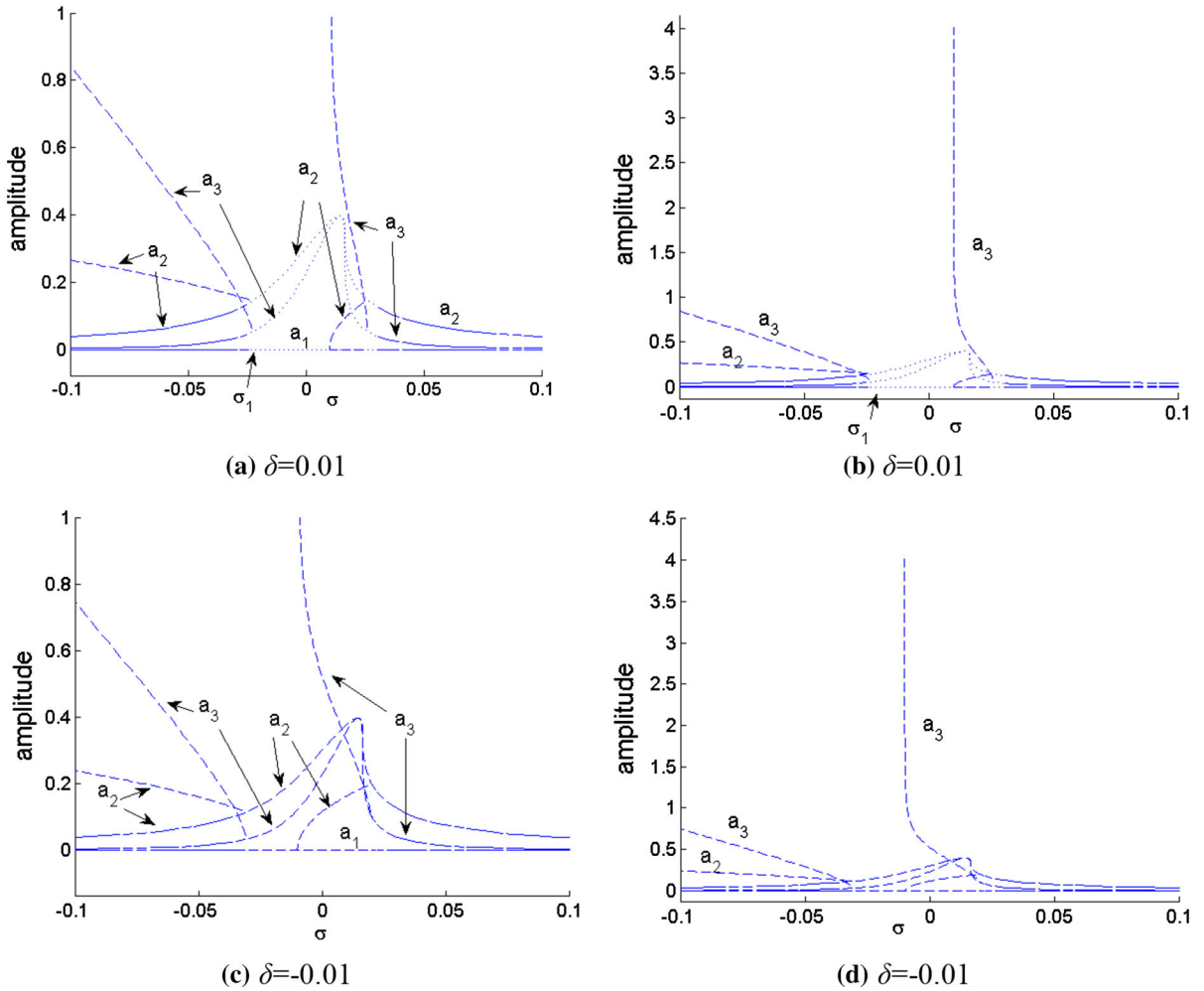


Fig. 14 Frequency-response curves for one-to-one internal resonance

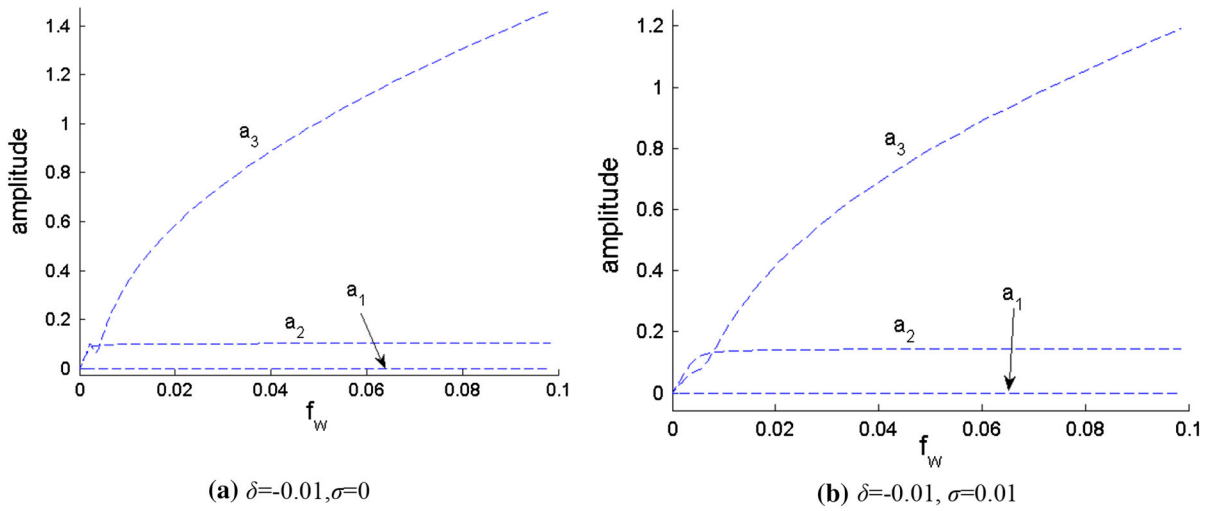


Fig. 15 Force–response curves for two-to-one internal resonance

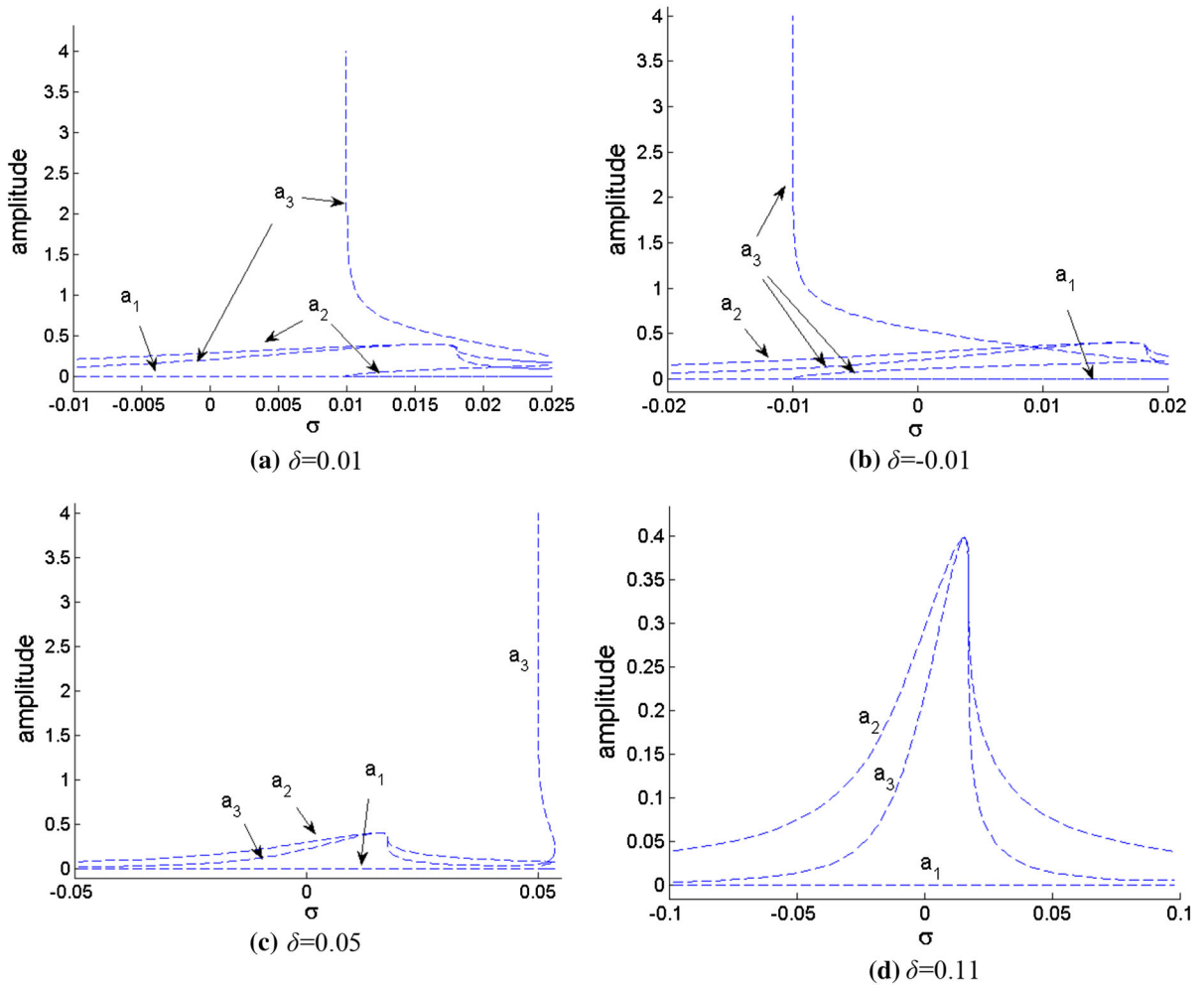


Fig. 16 Frequency–response curves for two-to-one internal resonance

## 8 Conclusions

As a widespread and promising technology, one profile of energy harvesting consists of exploiting nonlinear properties of vibrating structures for capturing useful energies provided by environmental sources or machines operation. Large amplitude forced vibration of a composite beam carrying a moving mass alongside is studied under harmonic base excitation. The moving mass, reciprocating inside a wire coil, is considered to act partially as a vibration absorber and also as electric generator through transforming mechanical into electrical energy. The composite beam is excited along the  $v$  or  $w$  directions, which brings induced motion to the sliding mass along the beam arc length due to second order effects. By properly applying conditions of internal resonance, optimal coupling can be set between the moving mass and the directly excited modes. By conducting bifurcation analyses, it is shown that the saturation phenomenon can be taken into advantage for diverging energy toward the axial direction and thereafter generating electricity. Present study reveals that such absorbers can be used successfully in order to attenuate nonplanar large amplitude beam vibrations by ingeniously exploiting the often undesired and complicating nonlinearities.

## Appendix

The complete form of the equations, referred by their equation number in the main text:

$$(cv_1)\ddot{V} + (cv_2)\dot{V} + (cv_3)V + (cv_4)E = \varepsilon \left\{ (cv_{n1})r\ddot{V} \right. \\ + (cv_{n2})EW + (cv_{n3})VW + (cv_{n4})\ddot{E}W \\ + (cv_{n5})\dot{E}\dot{W} + (cv_{n6})\ddot{r}V - (cv_{n7}k_s)rV \\ + (cv_{n8})\dot{r}\dot{V} + (cv_{w2v})W^2V + (cv_{E^2v})E^2V \\ + (cv_{v3})V^3 + (cv_{E3})E^3 + (cv_{EV2})EV^2 \\ + (cv_{EW2})EW^2 + (cv_{\ddot{v}w2})\ddot{V}W^2 \\ + 2(cv_{2\dot{v}\dot{w}w})\dot{V}\dot{W}W + (cv_{r2\ddot{v}})r^2\ddot{V} \\ + (cv_{r\dot{v}\dot{v}})r\dot{r}\dot{V} + (cv_{r\ddot{v}v})r\ddot{r}V + (cv_{r^2v})r^2V \\ + (cv_{\dot{r}2v})\dot{r}^2V + 2(cv_{LV})(V^2\ddot{V} + V\dot{V}^2) \\ \left. + 2(cv_{LW})(VW\ddot{W} + V\dot{W}^2) \right\},$$

$$+ \frac{1}{2} \left( \int_0^1 \phi_v(s)ds \right) (f_v\Omega_v^2) (e^{i\Omega_v T_0} + e^{-i\Omega_v T_0}) \Bigg\}, \quad (4.4)$$

$$(cw_1)\ddot{W} + (cw_2)\dot{W} + (cw_3)W = \varepsilon \left\{ (cw_{n1})r\ddot{W} \right. \\ + (cw_{n2})EV + (cw_{n3})\dot{E}\dot{V} + (cw_{n4})E^2 \\ + (cw_{n5})V^2 + (cw_{n6})\ddot{r}W - (cw_{n7}k_s)rW \\ + (cv_{r2\ddot{w}})r^2\ddot{W} + (cv_{r^2w})r^2W + (cv_{r\ddot{r}w})r\ddot{r}W \\ + (cv_{\dot{r}2w})\dot{r}^2W + (cv_{wv2})WV^2 + (cv_{w3})W^3 \\ + (cv_{w\dot{v}2})W\dot{V}^2 + (cv_{E^2w})E^2W \\ + (cv_{EVW})EVW + 2(cv_{LV})(VW\ddot{V} \\ + W\dot{V}^2) + 2(cv_{LW})(W^2\ddot{W} + W\dot{W}^2) \\ \left. + \frac{1}{2} \left( \int_0^1 \phi_w(s)ds \right) (f_w\Omega_w^2) (e^{i\Omega_w T_0} + e^{-i\Omega_w T_0}) \right\}, \quad (4.5)$$

$$(c\phi_1)\ddot{E} + (c\phi_2)\dot{E} + (c\phi_3)E + (c\phi_4)V \\ = \varepsilon \left\{ (c\phi_{n1})VW + (c\phi_{n2})EW + (c\phi_{n3})\ddot{V}W \right. \\ + (c\phi_{n4})\dot{V}\dot{W} + (c\phi_{E^2v})E^2V + (c\phi_{v3})V^3 \\ + (c\phi_{EV2})EV^2 + (c\phi_{EW2})EW^2 \\ \left. + \frac{1}{2} \left( \int_0^1 \phi_\phi(s)ds \right) (f_\phi\Omega_\phi^2) (e^{i\Omega_\phi T_0} + e^{-i\Omega_\phi T_0}) \right\}, \quad (4.6)$$

$$m_s\ddot{r} + k_s r - k_t\dot{q} = \varepsilon \{ (cr_{n1})V\ddot{V} + (cr_{n2})\dot{V}^2 \\ + (cr_{n3})W\ddot{W} + (cr_{n4})\dot{W}^2 + (cr_{rW2})rW^2 \\ + cr_{r\dot{v}2}(r\dot{V}^2) + cr_{r\dot{w}2}(r\dot{W}^2) \\ + cr_{rV\ddot{v}}(rV\ddot{V}) + cr_{rW\ddot{w}}(rW\ddot{W}) \}. \quad (4.7)$$

$$k_q\ddot{q} + \dot{q} + \varepsilon k_e\dot{r} = 0, \quad (4.8)$$

$$(cv_1)D_0^2V_1 + (cv_3)V_1 + (cv_4)E_1 = -2(cv_1)D_0D_1V_0 \\ - (cv_2)D_0V_0 + (cv_{n1})r_1D_0^2V_0 \\ + (cv_{n2})E_0W_0 + (cv_{n3})V_0W_0 + (cv_{n4})D_0^2E_0W_0 \\ + (cv_{n5})D_0E_0D_0W_0 + (cv_{n6})D_0^2r_0V_0 \\ - (cv_{n7}k_s)r_0V_0 + (cv_{n8})D_0r_0D_0V_0$$



$$\begin{aligned}
& + (cv_{w^2v})W_0^2V_0 + (cv_{E^2v})E_0^2V_0 + (cv_{V^3})V_0^3 \\
& + (cv_{E^3})E_0^3 + (cv_{EV^2})E_0V_0^2 + (cv_{EW^2})E_0W_0^2 \\
& + (cv_{\dot{V}W^2})D_0^2V_0W_0^2 + 2(cv_{2\dot{V}\dot{W}W})D_0V_0D_0W_0W_0 \\
& + (cv_{r^2\dot{V}})r_0^2D_0^2V_0 + (cv_{r\dot{V}})r_0D_0r_0D_0V_0 \\
& + (cv_{r\dot{V}})r_0D_0^2r_0V_0 + (cv_{r^2V})r_0^2V_0 \\
& + (cv_{\dot{r}^2V})(D_0r_0)^2V_0 + 2(cv_{LV}) \\
& + (V_0^2D_0^2V_0 + V_0(D_0V_0)^2)2(cv_{LW}) \\
& \times (V_0W_0D_0^2W_0 + V_0(D_0W_0)^2) \\
& + \frac{1}{2} \left( \int_0^1 \phi_v(s) ds \right) (f_v \Omega_v^2) (e^{i\Omega_v T_0} + e^{-i\Omega_v T_0}),
\end{aligned} \tag{5.11}$$

$$\begin{aligned}
(cw_1)D_0^2W_1 + (cw_3)W_1 & = -2D_0D_1W_0 - (cw_2)D_0W_0 \\
& + (cw_{n1})r_0D_0^2W_0 + (cw_{n2})E_0V_0 \\
& + (cw_{n3})D_0E_0D_0V_0 + (cw_{n4})E_0^2 + (cw_{n5})V_0^2 \\
& + (cw_{n6})D_0^2r_0W_0 - (cw_{n7}k_s)r_0W_0 \\
& + (cw_{r^2\dot{W}})r_0^2D_0^2W_0 + (cw_{r^2W})r_0^2W_0 \\
& + (cv_{r\dot{W}})r_0D_0^2r_0W_0 + (cv_{r^2W})(D_0r_0)^2W_0 \\
& + (cw_{WV^2})W_0V_0^2 + (cw_{W^3})W_0^3 \\
& + (cw_{W\dot{V}^2})W_0(D_0V_0)^2 + (cw_{E^2W})E_0^2W_0 \\
& + (cw_{EVW})E_0V_0W_0 + 2(cv_{LV})(V_0W_0D_0^2V_0 \\
& + W_0(D_0V_0)^2) + 2(cv_{LW})(W_0^2D_0^2W_0 + W_0(D_0W_0)^2) \\
& + \frac{1}{2} \left( \int_0^1 \phi_w(s) ds \right) (f_w \Omega_w^2) (e^{i\Omega_w T_0} + e^{-i\Omega_w T_0}),
\end{aligned} \tag{5.12}$$

$$\begin{aligned}
(c\phi_1)D_0^2E_1 + (c\phi_3)E_1 + (c\phi_4)V_1 & = -2D_0D_1E_0 \\
& - (c\phi_2)D_0E_0 + (c\phi_{n1})V_0W_0 + (c\phi_{n2})E_0W_0 \\
& + (c\phi_{n3})D_0^2V_0W_0 + (c\phi_{n4})D_0V_0D_0W_0 \\
& + (c\phi_{E^2V})E_0^2V_0 + (c\phi_{V^3})V_0^3 + (c\phi_{EV^2})E_0V_0^2 \\
& + (c\phi_{EW^2})E_0W_0^2 \\
& + \frac{1}{2} \left( \int_0^1 \phi_\phi(s) ds \right) (f_\phi \Omega_\phi^2) (e^{i\Omega_\phi T_0} + e^{-i\Omega_\phi T_0}),
\end{aligned} \tag{5.13}$$

$$\begin{aligned}
m_s D_0^2 r_1 + k_s r_1 - k_t D_0 q_1 & = (cr_{n1}) V_0 D_0^2 V_0 \\
& + (cr_{n2})(D_0 V_0)^2 + (cr_{n3}) W_0 D_0^2 W_0 \\
& + (cr_{n4})(D_0 W_0)^2 + (cr_{rW^2}) r_0 W_0^2 \\
& + (cr_{r\dot{V}^2})(r_0(D_0 V_0)^2) + (cr_{r\dot{W}^2})(r_0(D_0 W_0)^2) \\
& - 2m_s D_0 D_1 r_0 - k_t D_1 q_0 + (cr_{rW\dot{W}})(r_0 W_0 D_0^2 W_0) \\
& + (cr_{rV\dot{V}})(r_0 V_0 D_0^2 V_0).
\end{aligned} \tag{5.14}$$

$$k_q D_0^2 q_1 + D_0 q_1 = -2k_q D_0 D_1 q_0 - D_1 q_0 - k_e D_0 r_0, \tag{5.15}$$

$$\begin{aligned}
H_{vj}(s, t) = v''(s, t) & \left\{ m_s \ddot{u} + m_s \ddot{r} \left( 1 - \frac{v'^2}{2} + \frac{w'^2}{2} \right) \right. \\
& - 2m_s \dot{r} \dot{v}' v' + k_s r \left( 1 - \frac{v'^2}{2} + \frac{w'^2}{2} \right) \Bigg\}_{s=r(t)} \\
& - \left\{ m_s (\dot{v}' \dot{r}) + m_s \ddot{r} v' + m_s \dot{r} (\dot{r} v'' + \dot{v}') \right. \\
& \left. + k_s r (v' + v' w'^2) \right\} \delta(s - r(t))
\end{aligned} \tag{8.1}$$

$$\begin{aligned}
H_{wj}(s, t) = w''(s, t) & \left\{ m_s \ddot{u} + m_s \ddot{r} \left( 1 - \frac{v'^2}{2} + \frac{w'^2}{2} \right) \right. \\
& - 2m_s \dot{r} \dot{v}' v' + k_s r \left( 1 - \frac{v'^2}{2} + \frac{w'^2}{2} \right) \Bigg\}_{s=r(t)} \\
& - \left\{ m_s \dot{r} \dot{w}' - m_s \ddot{r} w' - m_s \dot{r} (\dot{r} w'' + \dot{w}') \right. \\
& \left. - k_s r \left( w' + \frac{v'^2}{2} w' \right) \right\} \delta(s - r(t))
\end{aligned} \tag{8.2}$$

$$\begin{aligned}
H_r(t) = & \left\{ -m_s \ddot{u} - 2m_s \dot{u} \dot{w}' w' - m_s \ddot{v} v' \right. \\
& \left. - m_s \dot{w} \dot{w}' - k_s r w'^2 \right\}_{s=r(t)}
\end{aligned} \tag{8.3}$$

$$\begin{aligned}
cv_1 & = \int_0^1 \phi_v^2(s) ds + J_\xi \int_0^1 \phi_v'^2(s) ds + m_s \phi_v(r_e), \quad cv_2 \\
& = c_v \int_0^1 \phi_v^2(s) ds, \quad cv_3 = \beta_{33} \int_0^1 \phi_v''^2(s) ds, \\
cv_4 & = \beta_{13} \int_0^1 \phi_\phi'(s) \phi_\phi''(s) ds, \quad cv_{n1} \\
& = -2m_s \phi_v(r_e) \phi_\phi'(r_e), \\
cv_{n2} & = \{ \phi_v \beta_{11} (\phi_\phi' \phi_\phi'')' - \phi_v (\beta_{22} - \beta_{33}) (\phi_\phi \phi_\phi'')' \\
& - \phi_\phi' \beta_{11} (\phi_\phi' \phi_\phi') + \phi_\phi' (\beta_{22} - \beta_{33}) (\phi_\phi \phi_\phi'') \}_{s=1}
\end{aligned}$$

$$\begin{aligned}
& -\beta_{11} \int_0^1 \phi_v (\phi'_\phi \phi'_w)'' ds \\
& + (\beta_{22} - \beta_{33}) \int_0^1 \phi_v (\phi_\phi \phi''_w)'' ds, cv_{n3} \\
& = \{\phi_v \beta_{13} (2\phi''_v \phi'_w)\}_{s=1} - \beta_{13} \int_0^1 \phi_v (2\phi''_v \phi'_w)'' ds, \\
cv_{n4} & = \{-\phi_v J_\xi (\phi_\phi \phi'_w)\}_{s=1} \\
& + J_\xi \int_0^1 \phi_v (\phi_\phi \phi'_w)' ds, cv_{n5} = cv_{n4}, \\
cv_{n6} & = m_s \int_0^1 \phi_v \phi''_v ds - m_s \phi_v(r_e) \phi'_v(r_e), cv_{n7} \\
& = -\int_0^1 \phi_v \phi''_v ds + \phi_v(r_e) \phi'_v(r_e), cv_{n8} \\
& = -2m_s \phi_v(r_e) \phi'_v(r_e), \quad (8.4) \\
cw_1 & = \int_0^1 \phi_w^2(s) ds + J_\eta \int_0^1 \phi_w'^2(s) ds + m_s \phi_w(r_e), cw_2 \\
& = c_w \int_0^1 \phi_w^2(s) ds, cw_3 = \beta_{22} \int_0^1 \phi_w''^2(s) ds, \\
cw_{n1} & = -2m_s \phi_w(r_e) \phi'_w(r_e), \\
cw_{n2} & = \{\phi_w \beta_{11} (\phi'_\phi \phi''_v) - \phi_w (\beta_{22} - \beta_{33}) (\phi_\phi \phi''_v)'\} \\
& + \phi'_w (\beta_{22} - \beta_{33}) (\phi_\phi \phi''_v)\}_{s=1} \\
& + \beta_{11} \int_0^1 \phi_w (\phi'_\phi \phi''_v)' ds \\
& + (\beta_{22} - \beta_{33}) \int_0^1 \phi_w (\phi_\phi \phi''_v)'' ds, cw_{n3} \\
& = \{\phi_w J_\xi (\phi_\phi \phi'_v)\}_{s=1} - J_\xi \int_0^1 \phi_w (\phi_\phi \phi'_v)' ds, \\
cw_{n4} & = \{\phi_w \beta_{13} (\phi_\phi \phi'_\phi)' - \phi'_w \beta_{13} \phi_\phi \phi'_\phi\}_{s=1} \\
& - \beta_{13} \int_0^1 \phi_w (\phi_\phi \phi'_\phi)'' ds,
\end{aligned}$$

$$\begin{aligned}
cw_{n5} & = \{-\phi_w \beta_{13} (\phi''_v)^2\}_{s=1} \\
& + \beta_{13} \int_0^1 \phi_w (\phi''_v)^2 ds, cw_{n6} \\
& = m_s \int_0^1 \phi_w \phi''_w ds + m_s \phi_w(r_e) \phi'_w(r_e), \\
cw_{n7} & = -\int_0^1 \phi_w \phi''_w ds - \phi_w(r_e) \phi'_w(r_e), cv_{n8} \\
& = -2m_s \phi_v(r_e) \phi'_v(r_e), \quad (8.5) \\
c\phi_1 & = J_\xi \int_0^1 \phi_\phi^2(s) ds, c\phi_2 = c_\phi \int_0^1 \phi_\phi^2(s) ds, c\phi_3 \\
& = \beta_{11} \int_0^1 \phi_\phi'^2(s) ds, \\
c\phi_4 & = \beta_{13} \int_0^1 \phi_v'^2(s) ds, c\phi_{n1} = \{-\phi_\phi \beta_{11} \phi''_v \phi'_w\}_{s=1} \\
& + \beta_{11} \int_0^1 \phi_\phi (\phi''_v \phi'_w)' ds + (\beta_{22} - \beta_{33}) \\
& \int_0^1 \phi_\phi (\phi''_v \phi''_w) ds, \\
c\phi_{n2} & = \{-\phi_\phi \beta_{13} (\phi_\phi \phi''_w)\}_{s=1} + \beta_{13} \int_0^1 \phi_\phi^2 \phi_w''' ds, c\phi_{n3} \\
& = -J_\xi \int_0^1 \phi_\phi \phi'_v \phi'_w ds, c\phi_{n4} = c\phi_{n3}, \quad (8.6) \\
cr_{n1} & = m_s \left( \int_0^s \phi_v'^2(s) ds \right)_{s=r_e} \\
& - m_s (\phi_v \phi'_v)_{s=r_e}, cr_{n2} \\
& = m_s \left( \int_0^s \phi_v'^2(s) ds \right)_{s=r_e}, \\
cr_{n3} & = m_s \left( \int_0^s \phi_w'^2(s) ds \right)_{s=r_e}
\end{aligned}$$

$$\begin{aligned}
& -m_s(\phi_w \phi'_w)_{s=r_e}, cr_{n4} \\
& = m_s \left( \int_0^s \phi_w'^2(s) ds \right)_{s=r_e}, \quad (8.7)
\end{aligned}$$

Coefficients of nonlinear cubic terms:

$$\begin{aligned}
cv_{W^2V} & = \{\phi_v \beta_{11}(\phi_w'^2 \phi''_v)' + \phi_v \beta_{33}(\phi'_v(\phi'_w \phi''_w)') \\
& - \phi'_v \beta_{11}(\phi''_v \phi_w'^2) + \phi'_v(\beta_{22} - \beta_{33})\phi'_v \phi'_w \phi''_w\}_{s=1} \\
& - \beta_{11} \int_0^1 \phi_v(\phi''_v \phi_w'^2)'' ds \\
& - \beta_{33} \int_0^1 \phi_v(\phi'_v(\phi'_w \phi''_w)')' ds, \\
cv_{E^2V} & = \{\phi_v(\beta_{22} - \beta_{33})(\phi_\phi^2 \phi''_v)'\} \\
& - \phi'_v(\beta_{22} - \beta_{33})(\phi_\phi^2 \phi''_v)\}_{s=1} \\
& - (\beta_{22} - \beta_{33}) \int_0^1 \phi_v(\phi_\phi^2 \phi''_v)'' ds,
\end{aligned}$$

$$\begin{aligned}
cv_{V^3} & = \{\phi_v \beta_{33}(\phi'_v(\phi'_v \phi''_v)')\}_{s=1} \\
& - \beta_{33} \int_0^1 \phi_v(\phi'_v(\phi'_v \phi''_v)')' ds,
\end{aligned}$$

$$\begin{aligned}
cv_{E^3} & = \{-\phi_v \beta_{13}(1/2)(\phi_\phi^2 \phi'_\phi)'\} \\
& + \phi'_v \beta_{13}(1/2)(\phi_\phi^2 \phi'_\phi)\}_{s=1} \\
& + \beta_{13}(1/2) \int_0^1 \phi_v(\phi_\phi^2 \phi'_\phi)'' ds,
\end{aligned}$$

$$\begin{aligned}
cv_{EV^2} & = \{\phi_v \beta_{13}(1/2)(\phi_v'^2 \phi''_\phi) \\
& - \phi'_v \beta_{13}(1/2)(\phi_v'^2 \phi''_\phi)\}_{s=1} \\
& - \beta_{13}(1/2) \int_0^1 \phi_v(\phi''_\phi \phi_v'^2)' ds,
\end{aligned}$$

$$\begin{aligned}
cv_{EW^2} & = \{\phi_v \beta_{13} \phi_\phi(\phi'_w \phi''_w)' - \phi'_v \beta_{13} \phi_\phi \phi'_w \phi''_w\}_{s=1} \\
& - \beta_{13} \int_0^1 \phi_v(\phi_\phi(\phi'_w \phi''_w)')' ds,
\end{aligned}$$

$$\begin{aligned}
cv_{\dot{V}W^2} & = \{-\phi_v J_\xi(\phi_w'^2 \phi'_v)\}_{s=1} \\
& + J_\xi \int_0^1 \phi_v(\phi_w'^2 \phi'_v)' ds, cv_{2\dot{V}W\dot{W}} = cv_{\dot{V}W^2}, \\
cv_{r^2\dot{V}} & = -m_s(\phi_v'^2)_{s=r_e}, cv_{r\dot{r}\dot{V}} \\
& = -2m_s(\phi_v \phi''_v + \phi_v'^2)_{s=r_e}, cv_{r\dot{r}V} = (cv_{r\dot{r}\dot{V}}/2), \\
cv_{r^2V} & = -k_s(\phi_v \phi''_v + \phi_v'^2)_{s=r_e}, cv_{\dot{r}^2V} \\
& = -m_s(\phi_v \phi''_v)_{s=r_e}, \\
cv_{LV} & = \int_0^1 \phi_v \phi''_v ds \left\{ -\frac{m_s}{2} \left( \int_0^s \phi_v'^2 ds \right)_{s=r_e} \right\} \\
& - \frac{1}{2} \int_0^1 \phi_v \left[ \phi'_v \int_1^s \int_0^s \phi_v'^2 ds ds \right]' ds, \\
cv_{LW} & = \int_0^1 \phi_v \phi''_v ds \left\{ -\frac{m_s}{2} \left( \int_0^s \phi_w'^2 ds \right)_{s=r_e} \right\} \\
& - \frac{1}{2} \int_0^1 \phi_v \left[ \phi'_v \int_1^s \int_0^s \phi_w'^2 ds ds \right]' ds, \quad (8.8)
\end{aligned}$$

$$\begin{aligned}
cw_{r^2\dot{W}} & = -m_s(\phi_w'^2)_{s=r_e}, cw_{r^2W} \\
& = k_s(\phi_w \phi''_w + \phi_w'^2)_{s=r_e}, cw_{r\dot{r}W} = \left(\frac{m_s}{k_s}\right) cw_{r^2W},
\end{aligned}$$

$$\begin{aligned}
cw_{\dot{r}^2W} & = m_s(\phi_w \phi''_w)_{s=r_e}, cw_{WV^2} \\
& = \{-\phi_w \beta_{11} \phi'_w \phi''_v + \phi_w \beta_{33} \phi'_w(\phi'_v \phi''_v)'\}_{s=1} \\
& + \beta_{11} \int_0^1 \phi_w(\phi'_w \phi''_v)' ds
\end{aligned}$$

$$- \beta_{33} \int_0^1 \phi_w[\phi'_w(\phi'_v \phi''_v)']' ds,$$

$$\begin{aligned}
cw_{W^3} & = \{\phi_w \beta_{22} \phi'_w(\phi'_w \phi''_w)'\}_{s=1} \\
& - \beta_{22} \int_0^1 \phi_w[\phi'_w(\phi'_w \phi''_w)']' ds,
\end{aligned}$$

$$cw_{W\dot{V}^2} = \{\phi_w J_\xi(\phi'_w \phi_v'^2)\}_{s=1} - J_\xi \int_0^1 \phi_w(\phi'_w \phi_v'^2)' ds,$$

$$\begin{aligned}
cw_{E^2W} & = \{-\phi_w(\beta_{22} - \beta_{33})(\phi_\phi^2 \phi''_w)'\} \\
& + \phi'_w(\beta_{22} - \beta_{33})(\phi_\phi^2 \phi''_w)\}_{s=1}
\end{aligned}$$

$$\begin{aligned}
& + (\beta_{22} - \beta_{33}) \int_0^1 \phi_w (\phi_\phi^2 \phi_w'')'' ds, \\
c_{wEVW} & = \{\phi_w \beta_{13} \phi_w' (\phi_\phi \phi_v')'' - \phi_w' \beta_{13} \phi_w' (\phi_\phi \phi_v')'\}_{s=1} \\
& - \beta_{13} \int_0^1 \phi_w [\phi_w' (\phi_\phi \phi_v')''] ds, \\
c_{wLv} & = \int_0^1 \phi_w \phi_w'' ds \left\{ -\frac{m_s}{2} \left( \int_0^s \phi_v'^2 ds \right) \right\}_{s=r_e} \\
& - \frac{1}{2} \int_0^1 \phi_w \left[ \phi_w' \int_1^s \int_0^s \phi_v'^2 ds ds \right]' ds, \\
c_{wLw} & = \int_0^1 \phi_w \phi_w'' ds \left\{ -\frac{m_s}{2} \left( \int_0^s \phi_w'^2 ds \right) \right\}_{s=r_e} \\
& - \frac{1}{2} \int_0^1 \phi_w \left[ \phi_w' \int_1^s \int_0^s \phi_w'^2 ds ds \right]' ds, \quad (8.9)
\end{aligned}$$

$$\begin{aligned}
c_{\phi E^2V} & = \{\phi_\phi \frac{1}{2} \beta_{13} (\phi_\phi^2 \phi_v'')\}_{s=1} \\
& - \frac{1}{2} \beta_{13} \int_0^1 \phi_\phi (\phi_\phi^2 \phi_v''') ds,
\end{aligned}$$

$$\begin{aligned}
c_{\phi V^3} & = \{-\phi_\phi \frac{1}{2} \beta_{13} (\phi_v'^2 \phi_v'')\}_{s=1} \\
& + \frac{1}{2} \beta_{13} \int_0^1 \phi_\phi (\phi_v'^2 \phi_v'')' ds,
\end{aligned}$$

$$\begin{aligned}
c_{\phi VW^2} & = \left\{ -\phi_\phi \frac{1}{2} \beta_{13} (\phi_v' \phi_w' \phi_w'') \right\}_{s=1} \\
& + \beta_{13} \int_0^1 \phi_\phi \phi_v' (\phi_w' \phi_w'')' ds,
\end{aligned}$$

$$\begin{aligned}
c_{\phi EV^2} & = -(\beta_{22} - \beta_{33}) \int_0^1 \phi_\phi^2 \phi_v''^2 ds, c_{\phi EW^2} \\
& = (\beta_{22} - \beta_{33}) \int_0^1 \phi_\phi^2 \phi_w''^2 ds, \quad (8.10)
\end{aligned}$$

$$\begin{aligned}
c_{r_r W^2} & = -k_s (\phi_w'^2)_{s=r_e}, c_{r_r \dot{V}^2} = m_s (\phi_v'^2)_{s=r_e}, \\
c_{r_r \dot{W}^2} & = m_s (\phi_v'^2)_{s=r_e}, \\
c_{r_r V \ddot{V}} & = -m_s (\phi_v \phi_v'')_{s=r_e}, c_{r_r W \ddot{W}} \\
& = -m_s (\phi_w \phi_w'')_{s=r_e}, \quad (8.11)
\end{aligned}$$

Coefficients of modulation equations:

$$\begin{aligned}
\Gamma_1 & = -cv_1 - \alpha c \phi_1, \\
\Gamma_2 & = \frac{(cv_2 + \alpha c \phi_2)}{2}, \\
\Gamma_3 & = -\omega^2 cv_{r^2 \ddot{V}} - \omega_r^2 cv_{r \ddot{V}} + cv_{r^2 V} + \omega_r^2 cv_{\dot{V}^2 V}, \\
\Gamma_4 & = cv_{W^2 V} + \alpha cv_{EW^2} - \omega^2 cv_{\ddot{V} W^2} \\
& + c\phi_{VW^2} + \alpha c\phi_{EW^2}, \\
\Gamma_5 & = \alpha^2 cv_{E^2 V} + cv_{V^3} + \alpha^3 cv_{E^3} + \alpha cv_{EV^2} \\
& - (4/3) \omega^2 cv_{LV} + \alpha^2 c\phi_{E^2 V} + c\phi_{V^3} + \alpha c\phi_{EV^2}, \\
\Gamma_6 & = -\omega^2 cv_{r^2 \ddot{V}} + \omega \omega_r cv_{r \ddot{V}} \\
& - \omega_r^2 cv_{r \ddot{V}} + cv_{r^2 V} - \omega_r^2 cv_{\dot{V}^2 V}, \\
\Gamma_7 & = -\omega^2 cv_{n1} - \omega_r^2 cv_{n6} - k_s cv_{n7} + \omega \omega_r cv_{n8}, \\
\Gamma_8 & = (1/2) f_v \Omega_v^2 \int_0^1 \phi_v(s) ds, \quad (8.12)
\end{aligned}$$

$$\begin{aligned}
\Lambda_1 & = -cw_1, \Lambda_2 = \frac{(cw_2)}{2}, \Lambda_3 = -\rho^2 cw_{r^2 \ddot{W}} \\
& + cw_{r^2 W} - \omega_r^2 cw_{r \ddot{W}} + \omega_r^2 cw_{\dot{W}^2 W}, \\
\Lambda_4 & = cw_{WV^2} + \omega^2 cw_{W \dot{V}^2} + \alpha^2 cw_{E^2 W} \\
& + \alpha cw_{EVW}, \Lambda_5 = cw_{W^3} - (4/3) \rho^2 cw_{LW}, \\
\Lambda_6 & = -\rho^2 cw_{r^2 \ddot{W}} + cw_{r^2 W} - \omega_r^2 cw_{r \ddot{W}} \\
& - \omega_r^2 cw_{\dot{W}^2 W}, \Lambda_7 = -\rho^2 cw_{n1} - \omega_r^2 cw_{n6} - k_s cw_{n7}, \\
\Lambda_8 & = \frac{f_w \Omega_w^2}{2} \int_0^1 \phi_w(s) ds, \quad (8.13)
\end{aligned}$$

$$\begin{aligned}
X_1 & = -m_s, X_2 = \omega^2 cr_{r \dot{V}^2} - \omega^2 cr_{r V \ddot{V}}, X_3 \\
& = \rho^2 cr_{r \dot{W}^2} + cr_{r W^2} - \rho^2 cr_{r W \ddot{W}}, \\
X_4 & = -\omega^2 cr_{r \dot{V}^2} - \omega^2 cr_{r V \ddot{V}}, X_5 \\
& = -\omega^2 cr_{n1} - \omega^2 cr_{n2}, \\
X_6 & = -\rho^2 cr_{r \dot{W}^2} + cr_{r W^2} - \rho^2 cr_{r W \ddot{W}}, X_7 \\
& = -\rho^2 cr_{n3} - \rho^2 cr_{n4}, \quad (8.14)
\end{aligned}$$

## References

1. Zavodney, L.D., Nayfeh, A.H.: The nonlinear response of a slender beam carrying a lumped mass to a principal parametric excitation: theory and experiment. *Int. J. Non-linear Mech.* **2**(24), 105–125 (1989)
2. Khalily, F., Golnaraghi, M.F., Heppler, G.R.: On the dynamic behavior of a flexible beam carrying a moving mass. *Nonlinear Dyn.* **5**, 493–513 (1994)
3. Ichikawa, M., Miyakawa, Y., Matsuda, A.: Vibration analysis of the continuous beam subjected to a moving mass. *J. Sound Vib.* **230**(3), 493–506 (2000)
4. Kononov, A.V., de Borst, R.: Instability analysis of vibrations of a uniformly moving mass in one and two-dimensional elastic systems. *Eur. J. Mech. A/Solids* **21**, 151–165 (2002)
5. Verichev, S.N., Metrikine, A.V.: Instability of vibrations of a mass that moves uniformly along a beam on a periodically inhomogeneous foundation. *J. Sound Vib.* **260**, 901–925 (2003)
6. Siddiqui, S.A.Q., Golnaraghi, M.F., Heppler, G.R.: Dynamics of a flexible cantilever beam carrying a moving mass. *Nonlinear Dyn.* **15**, 137–154 (1998)
7. Siddiqui, S.A.Q., Golnaraghi, M.F., Heppler, G.R.: Dynamics of a flexible beam carrying a moving mass using perturbation, numerical and time-frequency analysis techniques. *J. Sound Vib.* **229**(5), 1023–1055 (2000)
8. Siddiqui, S.A.Q., Golnaraghi, M.F., Heppler, G.R.: Large free vibrations of a beam carrying moving mass. *Int. J. Non-linear Mech.* **1**(38), 1481–1493 (2003)
9. Golnaraghi, M.F.: Vibration suppression of flexible structures using internal resonance. *Mech. Res. Commun. J.* **18**(2/3), 135–143 (1991)
10. Golnaraghi, M.F.: Regulation of flexible structures via nonlinear coupling. *J. Dyn. Control* **1**, 405–428 (1991)
11. Nayfeh, A.: *Nonlinear Interact.* Wiley, New York (2000)
12. Zhu, D., Tudor, M.J., et al.: Strategies for increasing the operating frequency range of vibration energy harvesters: a review. *Meas. Sci. Technol.* **21**(2), 1–29 (2010)
13. Barton, A.W., Burrow, S.G., Clare, L.R.: Energy harvesting from vibrations with a nonlinear oscillator. *J. Vib. Acoust.* **132**(2), 91–97 (2010)
14. Gammaitoni, L., Neri, I., Vocca, H.: Nonlinear oscillators for vibration energy harvesting. *Appl. Phys. Lett.* **94**(16), 164102 (2009)
15. Gammaitoni, L., Vocca, H., Neri, I., Travasso, F., Orfei, F.: In: Tan, Y.K. (ed.) *Vibration Energy Harvesting: Linear and Nonlinear Oscillator Approaches, Sustainable Energy Harvesting Technologies—Past, Present and Future.* ISBN: 978-953-307-438-2, InTech (2011)
16. C. Lee, D. Stamp, N.R. Kapania, Mur-Miranda, J.O.: Harvesting vibration energy using nonlinear oscillations of an electromagnetic inductor. In: *Proceedings of SPIE Energy Harvesting and Storage: Materials, Devices, and Applications* (2010); doi:[10.1117/12.849895](https://doi.org/10.1117/12.849895)
17. Abdelkefi, Abdessattar, Hajj, Muhammad R., Nayfeh, Ali H.: Power harvesting from transverse galloping of square cylinder. *Nonlinear Dyn.* **70**(2), 1355–1363 (2012)
18. Abdelkefi, A., Hajj, M.R., Nayfeh, A.H.: Phenomena and modeling of piezoelectric energy harvesting from freely oscillating cylinders. *Nonlinear Dyn.* **70**(2), 1377–1388 (2012)
19. Abdelkefi, A., Nayfeh, A.H., Hajj, M.R.: Design of piezoaeroelastic energy harvesters. *Nonlinear Dyn.* **68**(4), 519–530 (2012)
20. Abdelkefi, A., Nayfeh, A.H., Hajj, M.R.: Global nonlinear distributed-parameter model of parametrically excited piezoelectric energy harvesters. *Nonlinear Dyn.* **67**(2), 1147–1160 (2012)
21. Michael, I., Friswell, S.: Faruque Ali, vertical cantilever beam with tip mass. *J. Intell. Mater. Syst. Struct.* **23**(13), 1505–1521 (2012)
22. Pai, P.F., Nayfeh, A.H.: Three-dimensional nonlinear vibrations of composite beams-II. Flapwise excitations, nonlinear dynamics **2**, 1–34 (1991)
23. Pai, P.F., Nayfeh, A.H.: Three-dimensional nonlinear vibrations of composite Beams-III. Chordwise Excit. *Nonlinear Dyn.* **2**, 137–156 (1991)
24. Arafat, H.N.: *Non-linear response of cantilever beams*, Ph.D. Thesis, Virginia Polytechnic Institute and State University, Blacksburg, Virginia, (1999)
25. Nayfeh, A.H., Mook, D.T., Marshall, L.R.: Nonlinear coupling of pitch and roll modes in ship motion. *J. Hydronautics* **7**, 145–152 (1973)